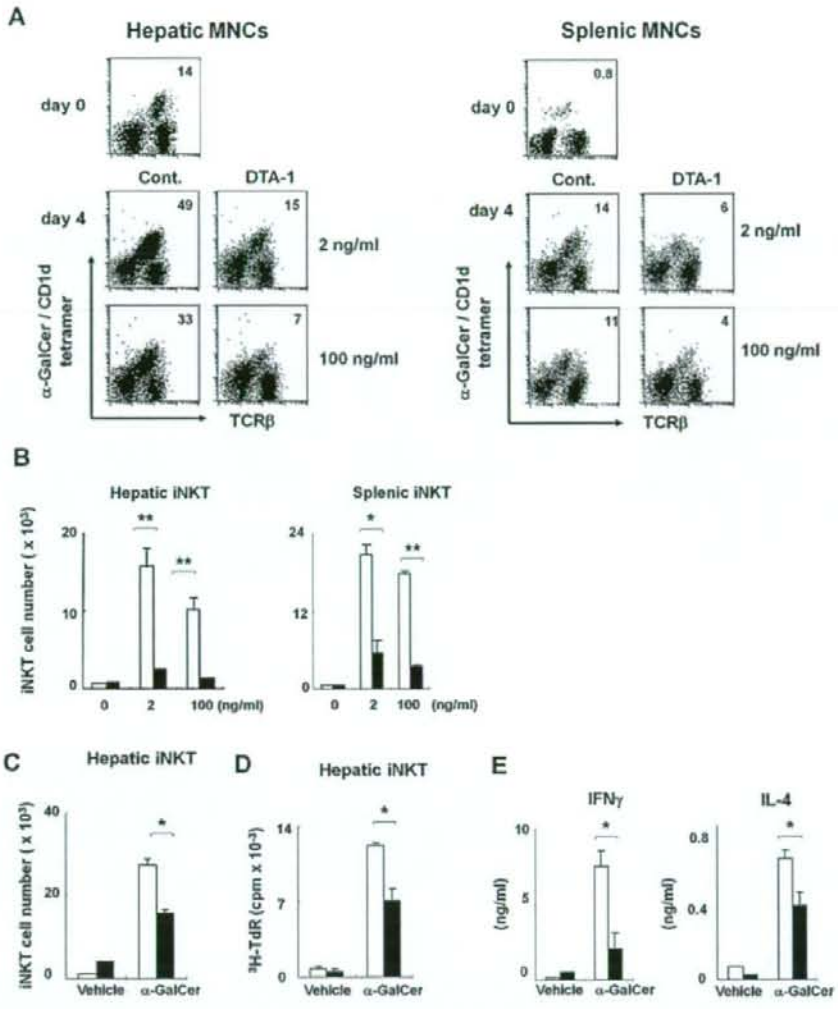

Figure 2. Agonistic anti-GITR mAb (DTA-1) inhibits α-GalCer-induced proliferation of iNKT cells, regardless of Ag dose and tissue origin. (A, B) MNC from the liver (5×10^6) (A) and spleen (2×10^5) (B) of WT mice were stimulated with higher dose (100 ng/mL) or lower dose (2 ng/mL) of α-GalCer in a 96-well round-bottom plate. Agonistic anti-GITR mAb (DTA-1; 10 μg/mL, ■) or control mAb (10 μg/mL, □) were added into the cell culture. At 4 days after stimulation, cells were stained with FITC-conjugated TCRβ and PE-conjugated α-GalCer/CD1d-tetramer and subjected to flow cytometry. (A) The frequency of TCRβ⁺ α-GalCer/CD1d-tetramer⁺ iNKT cells in the culture is shown. The results are representative of three mice in each genotypic group. (B) The numbers of TCRβ⁺ α-GalCer/CD1d-tetramer⁺ iNKT cells in the culture were counted. Results are expressed as the mean (± SD) of triplicate cultures. *$p<0.05$, **$p<0.01$. Similar results were obtained in five independent experiments. (C–E) Purified hepatic iNKT cells (1×10^5) were stimulated with 2 ng/mL α-GalCer in the presence of GITR-KO DC (1×10^5), which are unable to receive any GITR signals, in a 96-well round-bottom plate. Anti-GITR mAb (DTA-1, 10 μg/mL, ■) or control mAb (10 μg/mL, □) were added into the cell culture. (C) At 48 h after α-GalCer stimulation, the numbers of TCRβ⁺ α-GalCer/CD1d-tetramer⁺ iNKT cells in the culture were counted. Results are expressed as the mean (± SD) of triplicate cultures. (D) [³H]Thymidine incorporation during the last 4 h of the 96-h culture was measured and expressed as the mean (± SD) of triplicate cultures. *$p<0.05$. Similar results were obtained in three independent experiments. (E) The cell culture supernatants were collected 36 h after stimulation, and the cytokine levels in the supernatants were assayed for IFN-γ and IL-4. Results are expressed as the mean (± SD) of triplicate cultures. *$p<0.05$, **$p<0.01$. Similar results were obtained in two independent experiments.

GITR signals during Ag priming are critical for the inhibition of iNKT cell activation

We next asked whether stimulation of the GITR during Ag priming was sufficient for the GITR-mediated suppression of iNKT cell function, or whether sustained stimulation was required. To address this question, iNKT cells purified from the spleen of WT mice were stimulated with α-GalCer in the presence of GITR-KO DC for only the initial 24 h of culture, and then the number of live α-GalCer/CD1d-tetramer$^+$ TCRβ$^+$ iNKT cells was measured on the indicated days post stimulation. To provide GITR signals, the agonistic anti-GITR mAb was added for the initial 24 h, for the last 3 days, or for all 4 days. As shown in Fig. 3A and B, the engagement of GITR on iNKT cells during the initial 24 h (Ag-priming phase) significantly diminished the proliferation of iNKT cells, while the addition of anti-GITR mAb for the last 3 days, after the Ag was removed, had a negligible suppressive effect on iNKT cell proliferation. Therefore, GITR signals in iNKT cells during the Ag-priming phase are essential and sufficient for the suppression of iNKT cell activation.

Normal development of iNKT cells in GITR-deficient mice

To address the role of GITR in iNKT cell development, we next compared the frequency and absolute number of iNKT cells in the thymus, spleen, and liver between GITR-KO and WT mice. The percentage of α-GalCer/CD1d-tetramer$^+$ TCRβ$^+$ iNKT cells in these tissues was comparable in the WT and GITR-KO mice (Fig. 4A). The number of iNKT cells in the GITR-KO mice was not significantly different from that in WT mice (Fig. 4B). Further-

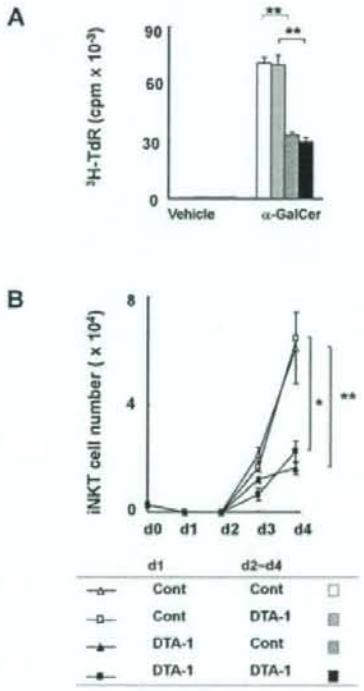

Figure 3. GITR signals during Ag priming are critical for the inhibition of iNKT cell activation. Purified WT iNKT cells (2×10^5) were α-GalCer-stimulated with GITR-KO DC (4×10^4) in the presence or absence of agonistic anti-GITR mAb as described in Fig. 2C. After 24 h of stimulation, the cells were washed and then cultured for an additional 3 days in the absence of α-GalCer. The agonistic anti-GITR mAb (DTA-1, 10 μg/mL) or control mAb (10 μg/mL) was added to the culture for the indicated days. (A) [^{3}H]Thymidine incorporation during the last 4 h of the 96-h culture was measured and expressed as the mean (± SD) of triplicate cultures. **$p<0.01$. (B) The numbers of live iNKT cells at the indicated days in the cell culture are demonstrated. Results are expressed as the mean (± SD) of triplicate cultures. *$p<0.05$, **$p<0.01$.

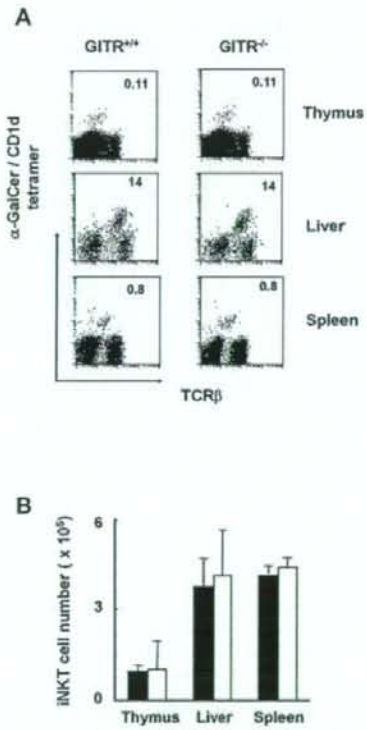

Figure 4. Normal development of iNKT cells in GITR-deficient mice. MNC isolated from the thymus, liver, and spleen of GITR-KO or WT mice were counted for cell numbers. The cells were stained with FITC-conjugated TCRβ, PE-conjugated α-GalCer/CD1d-tetramer and subjected to flow cytometry. (A) The frequency of the TCRβ$^+$ α-GalCer/CD1d-tetramer$^+$ iNKT cells in each tissue is shown. The results are representative of three mice in each genotypic group. (B) The numbers of TCRβ$^+$ α-GalCer/CD1d-tetramer$^+$ iNKT cells in the indicated tissues of GITR-KO (n=3, □) and WT (n=3, ■) mice were calculated from their frequency in MNC. Results are expressed as the mean (± SD).

more, the expression levels of iNKT-associated markers, such as CD4, CD69, Ly49A, and NKG2D, were similar between the GITR-KO and WT mice (data not shown). Collectively, these results show that, in spite of the significant expression of GITR on iNKT cells, GITR is dispensable for iNKT cell development.

GITR-KO iNKT cells show enhanced activation in response to Ag *in vitro*

We next examined *in vitro* proliferative response of α-GalCer/CD1d-tetramer$^+$ TCRβ$^+$ iNKT cells isolated from the liver of GITR-deficient mice. As shown in Fig. 5A, the recovery of GITR-KO iNKT cells after *in vitro* treatment with Ag (α-GalCer) was significantly higher than that from WT control iNKT cells. The DNA synthesis by GITR-KO iNKT cells upon Ag stimulation was also enhanced compared with that of WT controls (Fig. 5B). The culture supernatant of the purified iNKT cells from the liver of GITR-KO or WT mice was measured for IFN-γ and IL-4. Ag treatment caused a higher production of these cytokines in GITR-KO iNKT cells than in WT iNKT cells (Fig. 5C). These results are consistent with the observations using agonistic anti-GITR mAb, treatment of which suppresses the Ag-induced activation of iNKT cells.

Lack of GITR enhances iNKT cell activation *in vivo*

The *in vivo* effects of GITR signals on the Ag-induced iNKT cell activation were investigated. We injected α-GalCer i.p. into GITR-KO mice and examined the *in vivo* proliferation of α-GalCer/CD1d-tetramer$^+$ TCRβ$^+$ iNKT cells. Thymectomized mice were used to avoid the interfusion of newly differentiated naïve iNKT cells from the thymus. As expected, the number of the tetramer$^+$ iNKT cells was significantly increased in the liver and spleen of thymectomized GITR-deficient mice; the values were twice those seen in the thymectomized WT mice (Fig. 6A). Similar results were obtained when using a non-thymectomized mice combination (data not shown).

To address whether the increased number of Ag-activated iNKT cells in GITR-KO mice may be mediated by an apoptotic mechanism, we examined apoptosis of iNKT cells in the α-GalCer-treated thymectomized mice using Annexin V staining. Fig. 6B demonstrated that the intensity level for Annexin V staining after Ag stimulation between WT and GITR-KO iNKT cells were similar. Therefore, the increase in iNKT cell number seen in GITR-deficient mice is mainly mediated by cell proliferation rather than apoptosis.

We next examined cytokine secretion of GITR-KO iNKT cells during Ag-induced activation. The GITR-KO mice showed higher serum levels of IFN-γ and IL-4 upon i.p. injection with α-GalCer (Fig. 6C). *Ex vivo* intracellular cytokine staining demonstrated that Ag-stimulation induces higher production of IL-4 and IFN-γ by iNKT cells in GITR-deficient mice than in WT mice (Fig. 6D). Collectively, GITR deficiency promotes not only proliferation but also cytokine production of iNKT cells upon *in vivo* stimulation with α-GalCer.

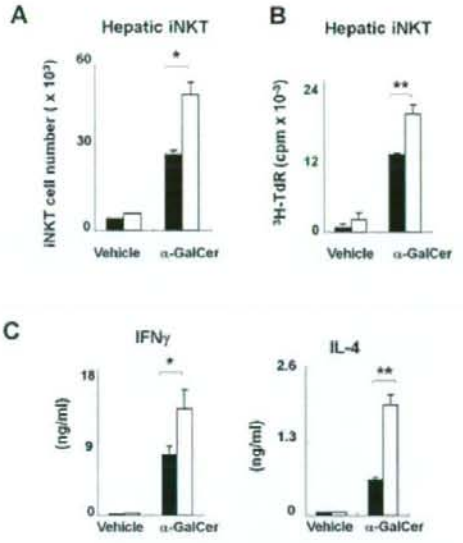

Figure 5. GITR-deficient iNKT cells show enhanced activation in response to Ag *in vitro*. Purified α-GalCer/CD1d-tetramer$^+$ iNKT cells from the liver of GITR-KO (□) or WT mice (■) were stimulated with α-GalCer (2 ng/mL) in the presence of GITR-KO DC as described in Fig. 2C. (A) The numbers of live iNKT cells 48 h after stimulation are demonstrated. Results are expressed as the mean (± SD) of triplicate cultures. *$p<0.05$. (B) [^{3}H]Thymidine incorporation during the last 4 h of the 48-h culture was measured as an indicator of cell proliferation and expressed as the mean (± SD) of triplicate cultures. *$p<0.05$, **$p<0.01$. Similar results were obtained in two independent experiments. (C) The cell culture supernatants were collected 36 h after stimulation, and the cytokine levels in the supernatants were assayed for IFN-γ and IL-4. Results are expressed as the mean (± SD) of triplicate cultures. *$p<0.05$, **$p<0.01$. Similar results were obtained in two independent experiments.

Lack of GITR enhances iNKT cell-mediated anti-tumor immunity

Finally, to evaluate the *in vivo* roles for GITR, we set up an *in vivo* experimental system in which iNKT cells mediate anti-tumor immunity. The *ex vivo* cytotoxic activity of hepatic MNC derived from α-GalCer-treated GITR-KO mice on EL-4 cells was significantly higher than that of hepatic MNC from α-GalCer-treated WT mice (Fig. 7A). EL-4 cells were injected i.v. and 600 ng α-GalCer or vehicle was injected i.p. into WT or GITR-deficient mice. Although both the WT and GITR-KO mice died from liver metastasis of the tumor cells by 14 days after tumor injection when vehicle alone was administered, all of the α-GalCer-treated mice were alive at 14 days (Fig. 7B). However, the prolonged survival of the α-GalCer-treated WT mice (median survival = 17 days) compared with that of the vehicle-treated mice (median survival = 14 days) did not reach statistical significance, probably because our experimental protocol used a dose of α-GalCer that was about tenfold less than the usual dosage for enhancing anti-tumor

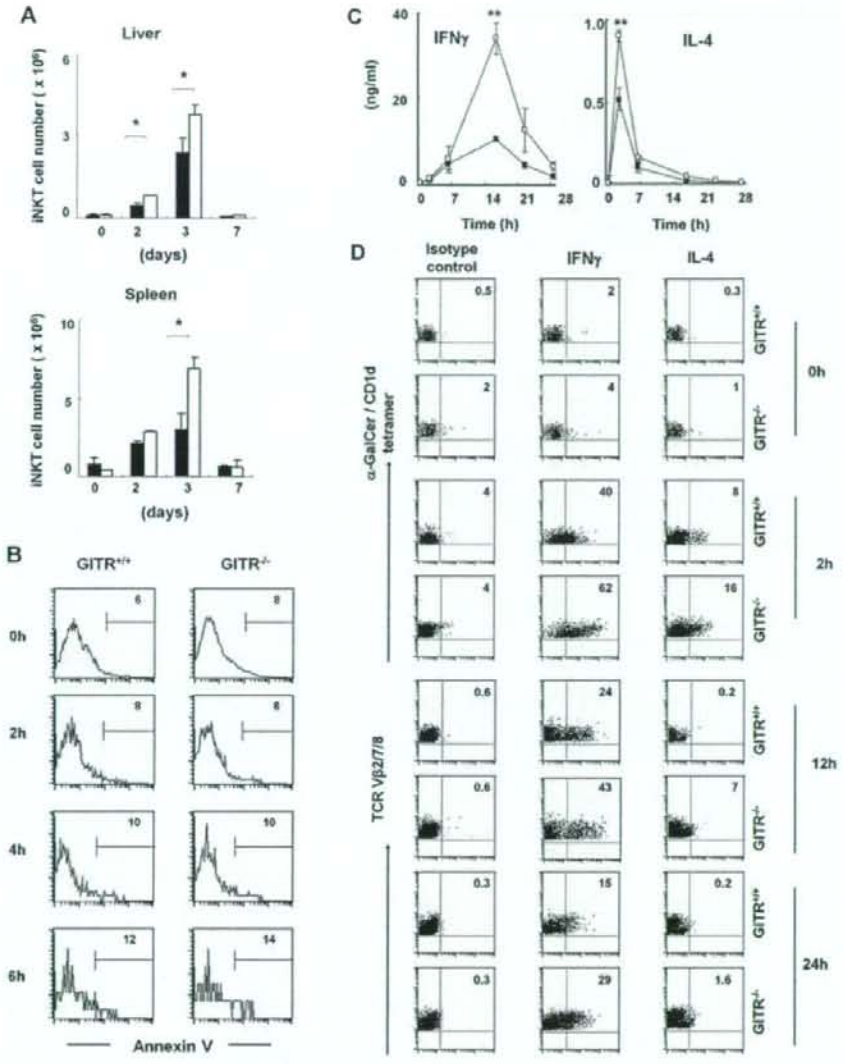

Figure 6. Lack of GITR promotes *in vivo* proliferation and cytokine production of iNKT cells. (A, B) Thymectomized GITR-KO (n=3, □) and WT (n=3, ■) mice were i.p. injected with 2 μg α-GalCer. (A) On days 2, 3 and 7 after injection, the absolute number of TCRβ$^+$ α-GalCer/CD1d-tetramer$^+$ iNKT cells in the liver and spleen of each mice are demonstrated. Results are expressed as the mean (± SD). *p<0.05. (B) Hepatic MNC were isolated from the thymectomized GITR-KO and WT mice at the indicated time after α-GalCer injection, and stained with allophycocyanin-conjugated Annexin V. The staining of electrically gated α-GalCer/CD1d-tetramer$^+$ TCRβ$^+$ cells in hepatic MNC is shown. The number shown in each panel represents the percentage of iNKT cells that were positive for Annexin V. (C, D) GITR-KO (n=3, □) and WT (n=3, ■) mice were i.p. injected with 2 μg α-GalCer. (C) Serum was collected at the indicated time for the cytokine measurement (IFN-γ and IL-4) by ELISA. Similar results were obtained in two independent experiments. (D) At 2, 12 and 24 h after α-GalCer stimulation, hepatic MNC were isolated, and cultured in the presence of Brefeldin A for 2 h without further stimulation. Intracellular staining of IFN-γ and IL-4 in α-GalCer /CDd tetramer$^+$ cells (0 and 2 h) and in TCR Vβ2/7/8$^+$ cells (12 and 24 h) was carried out. The number shown in each panel represents the percentage of iNKT cells that were positive for intracellular IFN-γ or IL-4. Similar results were obtained in three independent experiments.

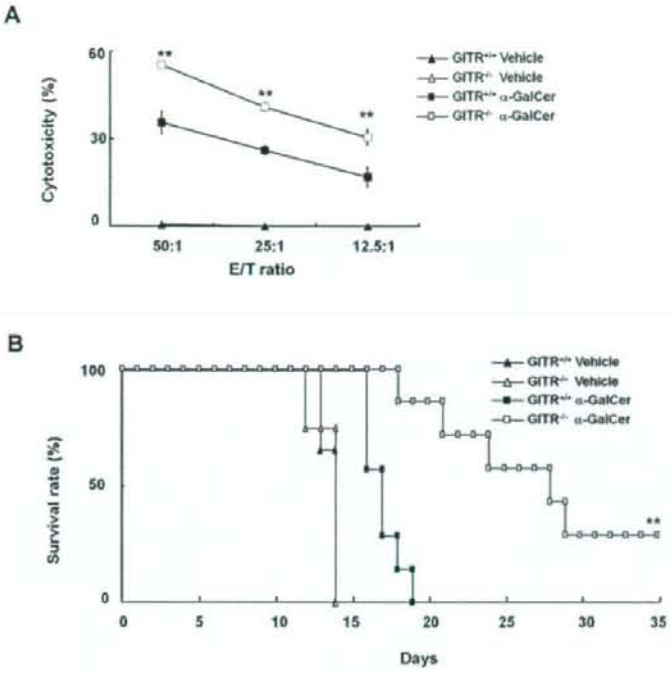

Figure 7. Lack of GITR promotes α-GalCer-mediated anti-tumor immunity. (A) Hepatic MNC were isolated from GITR-KO (□, △) and WT mice (n=3, ■, ▲) 24 h after the i.p. injection of α-GalCer (2 μg; □, ■) or vehicle (△, ▲), and incubated with ^{51}Cr-labeled EL-4 cells for 4 h. Radioactivities of the supernatants were determined with a γ-counter. Data shown are representative of three experiments. Results are expressed as the mean ± SD. *p<0.05. (B) EL-4 cells were injected i.v. into each mouse. On the same day, 600 ng α-GalCer (□, ■) or the same volume of vehicle (△, ▲) was injected i.p. The survival time of each mouse (n=7 in each group) was recorded. GITR-KO mice treated with α-GalCer (□) had significantly delayed mortality compared with α-GalCer-treated WT mice (■; log-rank **p<0.005).

immunity. In spite of the low α-GalCer dose, the α-GalCer was very effective in promoting the survival of the GITR-KO mice (median survival = 28 days, log-rank p<0.005). Taken together, these results indicate that GITR signals suppress the *in vivo* cytotoxic activity of iNKT cells for tumor cells.

Discussion

The present results suggest that signals through GITR can function as a negative regulator on iNKT cell activation in contrast to the positive roles of other costimulatory molecules including CD28, ICOS, CD40, and OX40 [15–17, 19, 22]. In addition, in spite of the down-regulation of TCR, NK cell receptors, and costimulatory molecules on the surface of recently activated iNKT cells, GITR expression is rather enhanced upon stimulation with α-GalCer (Fig. 1C). This suggests that recently activated iNKT cells are still ready to respond to GITR stimulation, but not to Ag or other costimulatory stimulation. The down-regulation of TCR and other costimulatory molecules might contribute to preventing over-activation of iNKT cells because CD28, ICOS and OX40 enhance iNKT cell activation [15–17, 19, 22]. The opposite function and expression profile of GITR to those of other costimulatory molecules suggest that GITR signals might play a role in counteracting the activation of iNKT cells to maintain homeostasis of iNKT cells.

GITR most closely resembles OX40 in the protein and gene structures and in immunological roles [6, 7, 27–32]. In addition, the genomes for OX40 and GITR might be evolutionarily derived from one gene because these genes are contiguously located on the same chromosomal locus, suggesting the redundant roles between OX40 and GITR. However, the effect of GITR signals in iNKT cells seems opposite to that of OX40. This conclusion may be supported by our preliminary results using GITR-OX40L-double KO mice. α-GalCer-induced iNKT cell proliferation and cytokine production in GITR-OX40L-double KO mice were reduced as compared with those in GITR-KO mice, but were much higher than those in OX40L-KO mice (our unpublished data). These results suggest that GITR and OX40 signals might be mutually nonredundant in iNKT cell function.

With regard to the suppressive functions of GITR in T cells, several findings have been reported. Tone *et al.* [9] have

demonstrated that GITR signals in the presence of high-dose Ag suppress T cell proliferation, while these signals in the presence of low-dose Ag promote the proliferation. Thus, we examined whether the effect of GITR signals differed in the presence of different Ag doses. In contrast to the case for T cells, similar suppressive effects by GITR were seen regardless of the Ag dose (Fig. 2, and data not shown). Although Tone *et al.* [9] suggest that *in vitro* GITR signals along with high-dose Ag may induce T cell apoptosis, which may lead to reduced T cell proliferation, we could not observe any difference in apoptosis between GITR-KO iNKT and WT iNKT cells after Ag stimulation (Fig. 6B). Thus, the mechanisms for the suppressive effects by GITR signals on T and iNKT cells might be different. On the other hand, a recent paper suggests that GITRL signals in DC induce suppressive immune responses through T cell and DC interaction. Since we used DC as APC *in vitro* cultures, signals through GITRL in DC might also contribute to the inhibition of iNKT cell function. To understand the mechanisms for the suppressive roles of GITR, further experimental evidence will be required.

One previous paper demonstrated that the engagement of GITR on NKT cell hybridomas and NK1.1$^+$ TCRβ$^+$ cells using agonistic anti-GITR mAb enhanced the cytokine production by these cells during activation [23]. These results appear to be the opposite of ours. However, Kim *et al.* [23] used the co-expression of NK1.1 and TCRβ as a marker for NKT cells. As mentioned in the introduction section, NK1.1$^+$ TCRβ$^+$ NKT cells may be a little different from α-GalCer/CD1d-tetramer$^+$ TCRβ$^+$ iNKT cells [3, 24], although some of these populations may overlap. Furthermore, the NK1.1$^+$ TCRβ$^+$ cells used in the previous study were stimulated with an anti-CD3 mAb instead of α-GalCer in most experiments [23]. Indeed, we failed to produce significant cell proliferation of α-GalCer/CD1d-tetramer$^+$ TCRβ$^+$ iNKT cells when anti-CD3 mAb was used according to the experimental procedure of Kim *et al.* (data not shown). In these contexts, the different results might be due to the difference in the NKT cell population used, and perhaps in the cell stimulation conditions. Nevertheless, our *in vivo* results using GITR-KO mice provide more specific evidence for GITR roles on α-GalCer/CD1d-tetramer$^+$ TCRβ$^+$ iNKT cell function.

Since the *in vivo* administration of α-GalCer or α-GalCer-treated DC effectively promotes anti-tumor immunity in mice, iNKT cells may be a promising target for anti-tumor therapies [3, 33]. Costimulatory signals through CD28, ICOS, and OX40 contribute to the cytokine production and cytotoxic activity of α-GalCer-activated iNKT cells [15–17, 19–22]. In addition, our results indicate that the lack of GITR signals enhances not only the cytokine production but also the proliferation of iNKT cells upon α-GalCer stimulation both *in vitro* and *in vivo*. Therefore, an *in vivo* blockade of GITR signals might induce the favorable anti-tumor effects mediated by iNKT cells, and could be augmented with protocols involving other stimulatory molecules, such as CD28, ICOS, and OX40. GITR might therefore be a useful target of immune therapies for cancer. In addition, several lines of evidence show the causative association of iNKT cell dysfunction with the development of autoimmune diabetes seen in NOD mice [34]. Enhancement of iNKT cell function by blocking GITR signals might also be a therapeutic strategy for autoimmune diseases in which impairment of iNKT cell function is involved. However, the deliberate engagement of GITR also leads to enhanced immune responses, such as autoimmunity and anti-tumor immunity, by breaking the regulatory T cell-mediated tolerance under certain conditions [35–40]. Therefore, the effects of GITR on immune responses may depend on the experimental conditions. Future studies will be necessary to elucidate the various roles of GITR in anti-tumor immunity.

Materials and methods

Mice

The GITR-deficient (GITR-KO) mice have been described previously [8]. WT mice were purchased from Japan SLC (Shizuoka, Japan). Age- (6–10 weeks old) and sex-matched WT mice were used as controls. All the mice were on a C57BL/6 background, and they were bred and maintained under specific-pathogen-free conditions. All procedures were performed according to the protocols approved by the Institutional Committee for Use and Care of Laboratory Animals of Tohoku University.

Cells

EL-4, a mouse T cell lymphoma line, was maintained in RPMI 1640 medium supplemented with 10% FBS, 100 U/mL penicillin, and 100 μg/mL streptomycin.

Ab and reagents

FITC-conjugated anti-TCRβ (H57–597), FITC-conjugated CD19 (1D3), PE-conjugated anti-Vβ2 TCR (B20.6), PE-conjugated anti-Vβ7 TCR (TR310), PE-conjugated anti-Vβ8 TCR (F23.1), biotin-conjugated anti-CD28 (37.51), biotin-conjugated anti-CD94 (18d3), biotin-conjugated anti-NKG2A (16a11), biotin-conjugated anti-ICOS (7E.17G9), biotin-conjugated anti-OX40 (OX86), allophycocyanin-conjugated anti-IFN-γ (XMG1.2), allophycocyanin-conjugated anti-IL-4 (11B11), and isotype control Ab were purchased from BD PharMingen (San Diego, CA). Purified, biotin- and allophycocyanin-conjugated anti-GITR mAb (DTA-1) were purchased from eBioscience (San Diego, CA). α-GalCer (KRN7000) was provided by Kirin Brewery (Gunma, Japan). Brefeldin A solution, allophycocyanin-conjugated Annexin V and 7-amino actinomycin (7AAD) were purchased from BD PharMingen.

Flow cytometry

To prevent nonspecific binding of Ab to FcRγ, cells were preincubated with anti-mouse CD16/32 (2.4G) before staining with specific Ab. Anti-TCRβ and α-GalCer/CD1d tetramer were used to detect iNKT cells as previously described [41]. In brief, cells were incubated with the indicated mAb and/or PE-conjugated α-GalCer/CD1d tetramer for 30 min at 4°C, then washed with PBS and analyzed with a FACSCalibur flow cytometer (BD Biosciences, Mountain View, CA). When using biotin-conjugated mAb, the cells were further incubated with PE- or allophycocyanin-conjugated streptavidin for 20 min. The analyses were conducted using the CellQuest program (BD Biosciences). To define iNKT cells at 24 h after α-GalCer stimulation, intracellular staining with the mixture of PE-conjugated anti-Vβ2, anti-Vβ7, and anti-Vβ8 TCR mAb was performed with a BD Cytofix/Cytoperm kit (BD Pharmingen) according to the manufacturer's instruction.

Purification of iNKT cells

Hepatic or splenic MNC were stained with FITC-conjugated anti-TCRβ and PE-conjugated α-GalCer/CD1d tetramer. The α-GalCer/CD1d-tetramer$^+$ TCRβ$^+$ cells were then sorted by a FACSAria cell sorter (BD Biosciences). The purity of the sorted cells was at least 95%.

Preparation of DC

Splenic DC were prepared as previously described [42]. In brief, the spleens of GITR-KO mice were treated with collagenase type III (400 U/mL; Sigma, St. Louis, MO) for 60 min at 37°C. The resulting single cells were incubated with CD11c MicroBeads (Miltenyi Biotec) for 15 min at 4°C. CD11c$^+$ cells were separated by an AutoMACS cell sorter (Miltenyi Biotec). The CD11c$^+$ fraction was typically ≥95% pure and used as DC (APC) for *in vitro* iNKT cell stimulation.

In vitro activation of iNKT cells

Hepatic (5×10^4) or splenic (2×10^5) MNC were stimulated with 2 ng/mL or 100 ng/mL α-GalCer for the indicated time in a 96-well round-bottom plate. Purified hepatic iNKT cells (1×10^5) were stimulated with 2 ng/mL α-GalCer in the presence of GITR-KO DC (APC; 1×10^5), which cannot receive any GITR signals. Splenic iNKT cells (2×10^3) were stimulated with 100 ng/mL α-GalCer in the presence of GITR-KO DC (4×10^4). To provide deliberate GITR signals, an agonistic anti-GITR mAb (DTA-1; 10 μg/mL) or control mAb was added to the culture. In some experiments, after 24 h of stimulation with α-GalCer, the cells were washed and cultured for an additional 3 or 4 days in the absence of α-GalCer. To measure proliferation incorporation of [^{3}H]thymidine in the cells was measured as previously described [43]. In brief, [^{3}H]thymidine (1 μCi/well) was added to 48- or 96-h cultures for the final 4 h at the time indicated. The mean incorporation of thymidine into DNA was measured as an indicator of cell proliferation and expressed as the mean (± SD) of triplicate cultures. Alternatively, cells were collected for flow cytometry at the indicated times. To detect cytokine production, the cell culture supernatants were collected 36 or 72 h after stimulation. The cytokine levels in the supernatants were assayed using ELISA kits for IFN-γ and IL-4 (BD Biosciences) according to the manufacturer's instruction.

Thymectomy

The upper part of the thoracic cavity of anesthetized mice was carefully opened to enable removal of the thymus with an aspirator. The wound was closed with surgical staples, and the mice were kept warm until fully recovered. The completeness of thymectomy was checked when the mouse was killed and those with remnants of thymus tissue were excluded from analysis. The thymectomized mice were subjected to *in vivo* experiments at least 3 weeks after thymectomy.

In vivo activation of iNKT cells

Mice were given i.p. injections of 2 μg α-GalCer. Serum was obtained at the indicated times, and the serum concentrations of IFN-γ and IL-4 were measured by ELISA. Intracellular staining of IFN-γ and IL-4 was carried out at 2, 12, and 24 h after α-GalCer injection. Briefly, MNC were isolated from the liver at the indicated time and cultured for 2 h in Brefeldin A without further stimulation. Surface labeling and intracellular staining were performed following the manufacturer's instruction (BD Cytofix/Cytoperm kit). On days 2, 3 and 7 after the α-GalCer injection, the number of live iNKT cells in the liver and spleen was calculated by counting the total cell number and frequency of α-GalCer/CD1d-tetramer$^+$ TCRβ$^+$ cells by flow cytometry. Apoptosis of iNKT cells was determined by Annexin V labeling at 2, 4, and 6 h after α-GalCer challenge. MNC were isolated from the liver at the indicated times and incubated with allophycocyanin-conjugated Annexin V in Annexin V binding buffer according to the manufacture's instruction. 7-amino actinomycin (7AAD) was added 10 min before acquisition to exclude dead cells.

Cytotoxicity assay

The cytolytic activity against NK-resistant EL-4 cells as target cells was assessed by a standard ^{51}Cr-release assay. As effector cells, hepatic MNC were collected from mice 24 h after i.p. injection with 2 μg α-GalCer. These cells were then incubated with ^{51}Cr-labeled EL-4 cells at the indicated ratios for 4 h. After the incubation, the radioactivity of the supernatants was determined with a γ-counter. The results were expressed as the % specific lysis

= [(release in test - spontaneous release) / (maximum release - spontaneous release)] × 100.

Tumor metastasis

EL-4 cells (4×10^5 cells in 0.2 mL) were injected into mice through the tail vein as described previously [44]. On the same day, 600 ng α-GalCer or the same volume of vehicle was injected i.p. The survival time of each mouse was recorded.

Statistic analysis

Statistical analyses were performed with Student's *t*-test. Values of $p<0.05$ were considered significant. Kaplan-Meier survival graphs were constructed and a log rank comparison of the groups was used to calculate the *p* values.

Acknowledgements: We would like to thank Dr. Kronenberg (La Jolla Institute, USA) for permitting use of the α-GalCer/CD1d-tetramer. This work was supported in part by a grant-in-aid for scientific research on priority areas from the Ministry of Education, Culture, Sports, Science and Technology of Japan, and a grant-in-aid for scientific research from the Japan Society for the Promotion of Science.

Conflict of interest: The authors declare no financial or commercial conflict of interest.

References

1 **Bendelac, A., Savage, P. B. and Teyton, L.,** The biology of NKT cells. *Annu. Rev. Immunol.* 2007. **25:** 297–336.

2 **Godfrey, D. I. and Berzins, S. P.,** Control points in NKT-cell development. *Nat. Rev. Immunol.* 2007. **7:** 505–518.

3 **Kronenberg, M.,** Toward an understanding of NKT cell biology: Progress and paradoxes. *Annu. Rev. Immunol.* 2005. **23:** 877–900.

4 **Nocentini, G. and Riccardi, C.,** GITR: A multifaceted regulator of immunity belonging to the tumor necrosis factor receptor superfamily. *Eur. J. Immunol.* 2005. **35:** 1016–1022.

5 **Shevach, E. M. and Stephens, G. L.,** The GITR-GITRL interaction: Co-stimulation or contrasuppression of regulatory activity? *Nat. Rev. Immunol.* 2006. **6:** 613–618.

6 **Ndhlovu, L. C., Takeda, I., Sugamura, K. and Ishii, N.,** Expanding role of T-cell costimulators in regulatory T-cell function: Recent advances in accessory molecules expressed on both regulatory and nonregulatory T cells. *Crit. Rev. Immunol.* 2004. **24:** 251–266.

7 **Watts, T. H.,** TNF/TNFR family members in costimulation of T cell responses. *Annu. Rev. Immunol.* 2005. **23:** 23–68.

8 **Ronchetti, S., Nocentini, G., Riccardi, C. and Pandolfi, P. P.,** Role of GITR in activation response of T lymphocytes. *Blood* 2002. **100:** 350–352.

9 **Tone, M., Tone, Y., Adams, E., Yates, S. F., Frewin, M. R., Cobbold, S. P. and Waldmann, H.,** Mouse glucocorticoid-induced tumor necrosis factor receptor ligand is costimulatory for T cells. *Proc. Natl. Acad. Sci. USA* 2003. **100:** 15059–15064.

10 **Muriglan, S. J., Ramirez-Montagut, T., Alpdogan, O., Van Huystee, T. W., Eng, J. M., Hubbard, V. M., Kochman, A. A. *et al.*,** GITR activation induces an opposite effect on alloreactive CD4(+) and CD8(+) T cells in graft-versus-host disease. *J. Exp. Med.* 2004. **200:** 149–157.

11 **Baltz, K. M., Krusch, M., Bringmann, A., Brossart, P., Mayer, F., Kloss, M., Baessler, T. *et al.*,** Cancer immunoediting by GITR (glucocorticoid-induced TNF-related protein) ligand in humans: NK cell/tumor cell interactions. *FASEB J.* 2007. **21:** 2442–2454.

12 **Liu, B., Li, Z., Mahesh, S. P., Pantanelli, S., Hwang, F. S., Siu, W. O. and Nussenblatt, R. B.,** Glucocorticoid-induced tumor necrosis factor receptor negatively regulates activation of human primary natural killer (NK) cells by blocking proliferative signals and increasing NK cell apoptosis. *J. Biol. Chem.* 2008. **283:** 8202–8210.

13 **Hanabuchi, S., Watanabe, N., Wang, Y. H., Ito, T., Shaw, J., Cao, W., Qin, F. X. and Liu, Y. J.,** Human plasmacytoid predendritic cells activate NK cells through glucocorticoid-induced tumor necrosis factor receptor-ligand (GITRL). *Blood* 2006. **107:** 3617–3623.

14 **Grohmann, U., Volpi, C., Fallarino, F., Bozza, S., Bianchi, R., Vacca, C., Orabona, C. *et al.*,** Reverse signaling through GITR ligand enables dexamethasone to activate IDO in allergy. *Nat. Med.* 2007. **13:** 579–586.

15 **Kawano, T., Cui, J., Koezuka, Y., Toura, I., Kaneko, Y., Motoki, K., Ueno, H. *et al.*,** CD1d-restricted and TCR-mediated activation of valpha14 NKT cells by glycosylceramides. *Science* 1997. **278:** 1626–1629.

16 **Hayakawa, Y., Takeda, K., Yagita, H., Van Kaer, L., Saiki, I. and Okumura, K.,** Differential regulation of Th1 and Th2 functions of NKT cells by CD28 and CD40 costimulatory pathways. *J. Immunol.* 2001. **166:** 6012–6018.

17 **Ikarashi, Y., Mikami, R., Bendelac, A., Terme, M., Chaput, N., Terada, M., Tursz, T. *et al.*,** Dendritic cell maturation overrules H-2D-mediated natural killer T (NKT) cell inhibition: Critical role for B7 in CD1d-dependent NKT cell interferon gamma production. *J. Exp. Med.* 2001. **194:** 1179–1186.

18 **Vinay, D. S., Choi, B. K., Bae, J. S., Kim, W. Y., Gebhardt, B. M. and Kwon, B. S.,** CD137-deficient mice have reduced NK/NKT cell numbers and function, are resistant to lipopolysaccharide-induced shock syndromes, and have lower IL-4 responses. *J. Immunol.* 2004. **173:** 4218–4229.

19 **Kaneda, H., Takeda, K., Ota, T., Kaduka, Y., Akiba, H., Ikarashi, Y., Wakasugi, H. *et al.*,** ICOS costimulates invariant NKT cell activation. *Biochem. Biophys. Res. Commun.* 2005. **327:** 201–207.

20 **Marschner, A., Rothenfusser, S., Hornung, V., Prell, D., Krug, A., Kerkmann, M., Wellisch, D. *et al.*,** CpG ODN enhance antigen-specific NKT cell activation *via* plasmacytoid dendritic cells. *Eur. J. Immunol.* 2005. **35:** 2347–2357.

21 **Uldrich, A. P., Crowe, N. Y., Kyparissoudis, K., Pellicci, D. G., Zhan, Y., Lew, A. M., Bouillet, P. *et al.*,** NKT cell stimulation with glycolipid antigen *in vivo*: Costimulation-dependent expansion, Bim-dependent contraction, and hyporesponsiveness to further antigenic challenge. *J. Immunol.* 2005. **175:** 3092–3101.

22 **Zaini, J., Andarini, S., Tahara, M., Saijo, Y., Ishii, N., Kawakami, K., Taniguchi, M. *et al.*,** OX40 ligand expressed by DCs costimulates NKT and $CD4^+$ Th cell antitumor immunity in mice. *J. Clin. Invest.* 2007. **117:** 3330–3338.

23 **Kim, H. J., Kim, H. Y., Kim, B. K., Kim, S. and Chung, D. H.,** Engagement of glucocorticoid-induced TNF receptor costimulates NKT cell activation *in vitro* and *in vivo*. *J. Immunol.* 2006. **176:** 3507–3515.

24 **Godfrey, D. I., MacDonald, H. R., Kronenberg, M., Smyth, M. J. and Van Kaer, L.,** NKT cells: What's in a name. *Nat. Rev. Immunol.* 2004. **4:** 231–237.

25 **Ota, T., Takeda, K., Akiba, H., Hayakawa, Y., Ogasawara, K., Ikarashi, Y., Miyake, S. *et al.***, IFN-gamma-mediated negative feedback regulation of NKT-cell function by CD94/NKG2. *Blood* 2005. **106:** 184–192.

26 **Wilson, M. T., Johansson, C., Olivares-Villagomez, D., Singh, A. K., Stanic, A. K., Wang, C. R., Joyce, S. *et al.***, The response of natural killer T cells to glycolipid antigens is characterized by surface receptor down-modulation and expansion. *Proc. Natl. Acad. Sci. USA* 2003. **100:** 10913–10918.

27 **Shimizu, J., Yamazaki, S., Takahashi, T., Ishida, Y. and Sakaguchi, S.**, Stimulation of CD25(+)CD4(+) regulatory T cells through GITR breaks immunological self-tolerance. *Nat. Immunol.* 2002. **3:** 135–142.

28 **Takeda, I., Ine, S., Killeen, N., Ndhlovu, L. C., Murata, K., Satomi, S., Sugamura, K. and Ishii, N.**, Distinct roles for the OX40-OX40 ligand interaction in regulatory and nonregulatory T cells. *J. Immunol.* 2004. **172:** 3580–3589.

29 **Sugamura, K., Ishii, N. and Weinberg, A. D.**, Therapeutic targeting of the effector T-cell co-stimulatory molecule OX40. *Nat. Rev. Immunol.* 2004. **4:** 420–431.

30 **Stephens, G. L., McHugh, R. S., Whitters, M. J., Young, D. A., Luxenberg, D., Carreno, B. M., Collins, M. and Shevach, E. M.**, Engagement of glucocorticoid-induced TNFR family-related receptor on effector T cells by its ligand mediates resistance to suppression by $CD4^+CD25^+$ T cells. *J. Immunol.* 2004. **173:** 5008–5020.

31 **Valzasina, B., Guiducci, C., Dislich, H., Killeen, N., Weinberg, A. D. and Colombo, M. P.**, Triggering of OX40 (CD134) on $CD4^+CD25^+$ T cells blocks their inhibitory activity: A novel regulatory role for OX40 and its comparison with GITR. *Blood* 2005. **105:** 2845–2851.

32 **Nocentini, G., Bartoli, A., Ronchetti, S., Giunchi, L., Cupelli, A., Delfino, D., Migliorati, G. and Riccardi, C.**, Gene structure and chromosomal assignment of mouse GITR, a member of the tumor necrosis factor/nerve growth factor receptor family. *DNA Cell Biol.* 2000. **19:** 205–217.

33 **Seino, K., Motohashi, S., Fujisawa, T., Nakayama, T. and Taniguchi, M.**, Natural killer T cell-mediated antitumor immune responses and their clinical applications. *Cancer Sci.* 2006. **97:** 807–812.

34 **Hussain, S., Wagner, M., Ly, D. and Delovitch, T. L.**, Role of regulatory invariant CD1d-restricted natural killer T-cells in protection against type 1 diabetes. *Immunol. Res.* 2005. **31:** 177–188.

35 **Turk, M. J., Guevara-Patino, J. A., Rizzuto, G. A., Engelhorn, M. E., Sakaguchi, S. and Houghton, A. N.**, Concomitant tumor immunity to a poorly immunogenic melanoma is prevented by regulatory T cells. *J. Exp. Med.* 2004. **200:** 771–782.

36 **Cohen, A. D., Diab, A., Perales, M. A., Wolchok, J. D., Rizzuto, G., Merghoub, T., Huggins, D. *et al.***, Agonist anti-GITR antibody enhances vaccine-induced CD8(+) T-cell responses and tumor immunity. *Cancer Res.* 2006. **66:** 4904–4912.

37 **Ramirez-Montagut, T., Chow, A., Hirschhorn-Cymerman, D., Terwey, T. H., Kochman, A. A., Lu, S., Miles, R. C. *et al.***, Glucocorticoid-induced TNF receptor family related gene activation overcomes tolerance/ignorance to melanoma differentiation antigens and enhances antitumor immunity. *J. Immunol.* 2006. **176:** 6434–6442.

38 **Calmels, B., Paul, S., Futin, N., Ledoux, C., Stoeckel, F. and Acres, B.**, Bypassing tumor-associated immune suppression with recombinant adenovirus constructs expressing membrane bound or secreted GITR-L. *Cancer Gene Ther.* 2005. **12:** 198–205.

39 **Wang, H. Y., Lee, D. A., Peng, G., Guo, Z., Li, Y., Kiniwa, Y., Shevach, E. M. and Wang, R. F.**, Tumor-specific human $CD4^+$ regulatory T cells and their ligands: Implications for immunotherapy. *Immunity* 2004. **20:** 107–118.

40 **Kohm, A. P., Williams, J. S. and Miller, S. D.**, Cutting edge: Ligation of the glucocorticoid-induced TNF receptor enhances autoreactive $CD4^+$ T cell activation and experimental autoimmune encephalomyelitis. *J. Immunol.* 2004. **172:** 4686–4690.

41 **Ikarashi, Y., Iizuka, A., Koshidaka, Y., Heike, Y., Takaue, Y., Yoshida, M., Kronenberg, M. and Wakasugi, H.**, Phenotypical and functional alterations during the expansion phase of invariant Valpha14 natural killer T (Valpha14i NKT) cells in mice primed with alpha-galactosylceramide. *Immunology* 2005. **116:** 30–37.

42 **Murata, K., Ishii, N., Takano, H., Miura, S., Ndhlovu, L. C., Nose, M., Noda, T. and Sugamura, K.**, Impairment of antigen-presenting cell function in mice lacking expression of OX40 ligand. *J. Exp. Med.* 2000. **191:** 365–374.

43 **Chen, S., Ishii, N., Ine, S., Ikeda, S., Fujimura, T., Ndhlovu, L. C., Soroosh, P. *et al.***, Regulatory T cell-like activity of $Foxp3^+$ adult T cell leukemia cells. *Int. Immunol.* 2006. **18:** 269–277.

44 **Takeda, K., Seki, S., Ogasawara, K., Anzai, R., Hashimoto, W., Sugiura, K., Takahashi, M. *et al.***, Liver $NK1.1^+$ $CD4^+$ alpha beta T cells activated by IL-12 as a major effector in inhibition of experimental tumor metastasis. *J. Immunol.* 1996. **156:** 3366–3373.

Abbreviations: **α-GalCer:** α-galactosylceramide · **GITR:** glucocorticoid-induced TNF receptor · **iNKT cell:** invariant natural killer T cell · **MNC:** mononuclear cells

Full correspondence: Dr. Naoto Ishii, Department of Microbiology and Immunology, Tohoku University Graduate School of Medicine, 2-1 Seiryo-machi, Aoba-ku, Sendai 980-8575, Japan
Fax: +81-22-717-8097
e-mail: ishiin@mail.tains.tohoku.ac.jp

Current addresses: Dr. Lishomwa C. Ndhlovu, Division of Experimental Medicine, Department of Medicine, San Francisco General Hospital, University of California, San Francisco, San Francisco, CA, USA

Received: 20/1/08
Revised: 23/4/08
Accepted: 11/6/08

Immunology
The Journal of cells, molecules, systems and technologies
British Society for immunology

IMMUNOLOGY ORIGINAL ARTICLE

Role of 2B4-mediated signals in the pathogenesis of a murine hepatitis model independent of Fas and Vα14 NKT cells

Hiroshi Furukawa,[1,2]
Hiroshi Kitazawa,[1] Izumi Kaneko,[1]
Mitsunobu Matsubara,[3]
Masato Nose[4] and Masao Ono[1]

[1]*Department of Pathology, Tohoku University Graduate School of Medicine, Sendai,* [2]*Department of Rheumatology, Clinical Research Center for Allergy and Rheumatology, Sagamihara National Hospital, National Hospital Organization, Sagamihara,* [3]*Division of Molecular Medicine, Center for Translational and Advanced Animal Research, Tohoku University Graduate School of Medicine, Sendai, and* [4]*Department of Pathology, Ehime University School of Medicine, Toon, Japan*

doi:10.1111/j.1365-2567.2008.02936.x
Received 17 June 2008; revised 24 July 2008; accepted 25 July 2008.
Correspondence: H. Furukawa, Department of Pathology, Tohoku University Graduate School of Medicine, Seiryo-machi 2-1, Aoba-ku, Sendai-shi, Japan 980-8575.
Email: hfurukawa@mail.tains.tohoku.ac.jp
Senior author: Masao Ono,
email: onomasao@mail.tains.tohoku.ac.jp

Summary

Concanavalin A (Con A)-induced hepatitis is a T-cell-mediated murine experimental model of autoimmune hepatitis. Mice lacking Vα14 NKT cells were found to be less sensitive to this hepatitis and the MRL/Mp-*Fas*$^{lpr/lpr}$ (MRL/lpr; i.e. Fas deficient) mice were also less sensitive. We report herein that MRL/Mp-*Fas*$^{lpr/lpr}$-*Sap*$^{rpl/-}$ (MRL/lpr/rpl) mice lack Vα14 NKT cells and are deficient in the Fas antigen but sensitive to Con A-induced hepatitis. The signaling lymphocytic activation molecule (SLAM)-associated protein (SAP) is an adaptor molecule containing a Src homology 2 (SH2) domain. We previously reported new mutant mice found among MRL/lpr mice and revealed that SAP deficiency led to the regression of autoimmune phenotypes in mutant MRL/lpr/rpl mice. It was also revealed that $CD4^+$ and $CD8^+$ T cells were effector cells and that blockade of 2B4, one of the SLAM family receptors, inhibited the induction of hepatitis in MRL/lpr/rpl mice. These data suggest that signals mediated by molecules other than SAP from 2B4 in T cells played important roles in the induction of hepatitis in MRL/lpr/rpl mice.

Keywords: 2B4; concanavalin A-induced hepatitis; Fas; SAP; SLAM family receptors

Introduction

Signaling lymphocytic activation molecule (SLAM)-associated protein (SAP) is an adaptor molecule containing a Src homology 2 (SH2) domain. SAP is expressed in T and natural killer (NK) cells and binds to the cytoplasmic domains of SLAM family receptors, resulting in the subsequent recruitment of Fyn.[1] The *SAP* gene is located on the X chromosome and is responsible for X-linked lymphoproliferative disease (XLP).[2] Patients with XLP disease are highly susceptible to the Epstein–Barr virus infection and suffer from infectious mononucleosis, malignant lymphoma and hypergammaglobulinaemia or hypogammaglobulinaemia. This SAP-mediated signal is essential for the development of NKT cells (i.e. unconventional CD1d-restricted T cells with invariant Vα14 T-cell receptors).[3] These Vα14 NKT cells recognize glycolipid antigens on CD1d molecules, such as α-galactosylceramide (α-GalCer) derived from a marine sponge or endogenous isoglobotrihexosyl ceramide, and secrete massive amounts of interleukin (IL)-4 and interferon-γ (IFN-γ).[4,5]

Abbreviations: α-GalCer, α-galactosylceramide; Con A, concanavalin A; EAT-2, Ewing's sarcoma-activated transcript-2; ELISA, enzyme-linked immunosorbent assay; ERT, EAT-2-related transducer; FasL, Fas ligand; GOT, glutamate oxalate transaminase; GPT, glutamic pyruvic transaminase; IFN-γ, interferon-γ; IL, interleukin; mAb, monoclonal antibody; NK, natural killer; PBS, phosphate-buffered saline; RT-PCR, reverse transcription-polymerase chain reaction; SAP, SLAM-associated protein; SH2, Src homology 2; SLAM, signaling lymphocytic activation molecule; TNF-α, tumour necrosis factor-α; XLP, X-linked lymphoproliferative disease.

Concanavalin A (Con A)-induced hepatitis is a murine experimental model of autoimmune hepatitis. Systemic injection of the plant lectin causes haemagglutination; activation of lymphocytes; secretion of cytokines such as tumour necrosis factor-α (TNF-α), IL-6, IFN-γ and IL-4; and subsequent hepatocyte injury.[6] Severe combined immunodeficiency mice and athymic mice are less sensitive to Con A-induced hepatitis, indicating that T cells are involved in hepatitis. This phenomenon is also known to be dependent on the Fas–Fas ligand (FasL) axis and Vα14 NKT cells.[7–9] Several studies have reported that molecules involved in Con A-induced hepatitis are P-selectin, LIGHT (homologous to lymphotoxin, exhibits inducible expression and competes with HSV glycoprotein D for herpes virus entry mediator, a receptor expressed by T lymphocytes), osteopontin, IL-4, IFN-γ and CD1d.[8–14]

The Fas antigen is a member of the TNF superfamily and mediates signals that induce apoptotic cell death. The MRL/Mp-*Fas*$^{lpr/lpr}$ (MRL/lpr) strain, in which the *Fas* gene is disrupted by the insertion of a retroposon, is a lupus-prone strain.[15,16] MRL/lpr mice show severe lymphadenopathy and splenomegaly as a result of the abnormal expansion of *lpr* T cells, $CD4^-$ $CD8^-$ $B220^+$ $Thy1.2^+$ αβ T cells. We previously reported new mutant mice found among the MRL/lpr mice and revealed that SAP deficiency regresses the autoimmune phenotypes in the mutant mice MRL/Mp-*Fas*$^{lpr/lpr}$-*Sap*$^{rpl/-}$ (MRL/lpr/rpl).[17] It was reported that MRL/lpr mice are less sensitive to Con A-induced hepatitis.[7] Furthermore, SAP-deficient mice were thought to be less sensitive to Con A-induced hepatitis because they lack Vα14 NKT cells.[3] Here, we report that MRL/lpr/rpl mice are sensitive to Con A-induced hepatitis and attempted to shed light on the mechanisms underlying this paradoxical Con A-induced hepatitis in MRL/lpr/rpl mice, which is independent of Fas and Vα14 NKT cells.

Materials and methods

Mice, cells and reagents

MRL mice were bred under specific pathogen-free conditions in Tohoku University. MRL/+ and MRL/lpr mice were purchased from Charles River Japan (Tokyo, Japan). MRL/lpr/rpl mice have previously been described.[17] The MRL/+/rpl mice were generated by crossing the MRL/+ mice with the MRL/lpr/rpl mice and by subsequent intercrossing of the resulting heterozygous F_1 mice. The F_2 mice were genotyped using the following primer sets: 5′-GAGAAGCTCTTACTCGGTA and 5′-CCACTACCAC GAGATATACT with *Kpn*I digestion for *rpl*; and 5′-GTA AATAATTGTGCTTCGTCAG, 5′-TAGAAAGGTGCACG GGTGTG and 5′-CAAATCTAGGCATTAACAGTG for the *lpr* loci. In all animal experiments, we adhered to the Tohoku University guidelines for animal experiments. Hybridoma cells for anti-CD4 (GK1·5) or anti-CD8 (53-6·72) monoclonal antibodies (mAbs) were provided by Tohoku University, Institute of Development, Aging and Cancer, Cell Resource Center for Biomedical Research. Antibody to asialo GM1 and antibody to Con A were purchased from Wako Pure Chemical Industries (Osaka, Japan). α-GalCer was provided by KIRIN brewery (Gunma, Japan). The other mAbs were purchased from BD Bioscience (Franklin Lakes, NJ).

Con A-induced hepatitis

We used five mice per group for all Con A-induced hepatitis experiments. Con A was dissolved in phosphate-buffered saline (PBS) and 200 μl of the solution was injected intravenously into the tail vein of MRL mice. Plasma glutamate oxalate transaminase (GOT) and glutamic pyruvic transaminase (GPT) levels were monitored 12 hr after the injection using a Fuji Drichem 3500v (Fuji film Co., Tokyo, Japan) with slides of GOT/AST-PIII and GPT/ALT-PIII, according to the manufacturer's instructions. $CD4^+$ or $CD8^+$ T cells, or NK cells, were depleted using monoclonal anti-CD4 or anti-CD8 or anti-asialo GM1, respectively, 3, 2 and 1 day before injection of Con A. The depletion efficiency was confirmed in the peripheral blood using a FACSCalbur flow cytometer (BD Bioscience). Serum levels of IL-4 were measured using enzyme-linked immunosorbent assay (ELISA) (BD Bioscience), according to the manufacturer's instructions.

Histological analysis

Autopsy was performed 12 hr after induction of hepatitis in MRL mice by 25 mg/kg of Con A. Organs from mice were fixed in 10% formalin in 0·01 M phosphate buffer (pH 7·2), embedded in paraffin and cut into sections. The sections were stained with hematoxylin and eosin.

Reverse transcription–polymerase chain reaction and vectors

Total RNA was isolated from MRL/+ splenocytes using Trizol (Invitrogen, Carlsbad, CA). cDNA was synthesized from 5 μg of total RNA using Superscript III (Invitrogen), according to the manufacturer's instructions. Reverse transcription–polymerase chain reaction (RT-PCR) was performed using KOD plus DNA polymerase (Toyobo, Osaka, Japan). The PCR products were subcloned into the sequence vector pCR4Blunt (Invitrogen). The sequences of the inserts were confirmed using BigDye Terminator v3.1 and the ABI Prism 3100 sequencer (Applied Biosystems, Foster City, CA). The expression vector pcDNA3·1A was purchased from Invitrogen. The fragments of the murine immunoglobulin G3 (IgG3) Fc region-FLAG and extracellular domains of the

SLAM family receptors (SLAM, 2B4, CD48, Ly9, CD84 and Ly108) were subcloned into pcDNA3·1A to generate the pcDNASLAMFc, pcDNA2B4Fc, pcDNACD48Fc, pcDNALy9Fc, pcDNACD84Fc and pcDNALy108Fc plasmids.

Hydrodynamics-based gene transfer and ELISA for detection of the Fc fusion protein

For *in vivo* gene expression, hydrodynamic injection of plasmids was performed.[14] Plasmids (10 μg) in 4 ml of lactated Ringer solution were rapidly injected into the tail vein of mice. The expression of the Fc fusion protein in the plasma was confirmed by ELISA. ELISA plates (F96 MAXISORP; Nunc, Roskilde, Denmark) were coated with 10 μg/ml of rabbit anti-FLAG (Sigma, St Louis, MO) in carbonate buffer (15 mM Na_2CO_3, 35 mM $NaHCO_3$) and blocked with 5% skim milk in PBS. After plasma samples were loaded, the fusion protein levels were detected with horseradish peroxidase-labelled rabbit anti-mouse IgG3 (1:5000 dilution; Rockland Immunochemicals, Gilbertsville, PA) and 3,3′,5,5′-tetramethylbenzidine peroxidase substrate (Moss, Inc., Pasadena, MD).

Flow cytometric analysis

Hepatic mononuclear cells were isolated as previously described.[18] Briefly, the liver was pressed through a 70-μm cell strainer (BD Bioscience). Hepatocytes were pelleted by centrifugation at 30 *g* for 3 min. The remaining liver cells in the supernatant were pelleted at 300 *g* for 5 min and then resuspended in a 40% isotonic Percoll solution (GE Healthcare Bioscience, Uppsala, Sweden). The suspension was underlaid with a 60% isotonic Percoll solution. After centrifugation at 1500 *g* for 20 min, mononuclear cells were isolated at the interface. The cells were stained with murine CD1d:Ig (BD Bioscience)-α-GalCer, according to the manufacturer's instructions, and analyzed using a FACSCalibur flow cytometer (BD Bioscience).

Results

MRL/lpr/rpl mice are more susceptible to Con A-induced hepatitis than MRL/lpr mice.

When 21 mg/kg of Con A was intravenously injected into MRL/+ mice, severe hepatitis was induced (Fig. 1a and c); the extent of hepatitis was evaluated by measuring the activities of the two deviation enzymes GOT and GPT and the survival rate. As reported previously,[7] MRL/lpr mice were less sensitive to Con A-induced hepatitis than MRL/+ mice (Fig. 1a,c). However, severe hepatitis was induced in MRL/+ and MRL/lpr/rpl mice when 27 mg/kg of Con A was injected (Fig. 1b,d). These findings were also confirmed by histological analysis. Severe zonal necrosis of hepatocytes was observed in the livers of MRL/+ and MRL/lpr/rpl mice but not in the livers of MRL/lpr mice (Fig. 2). These histological data correlated

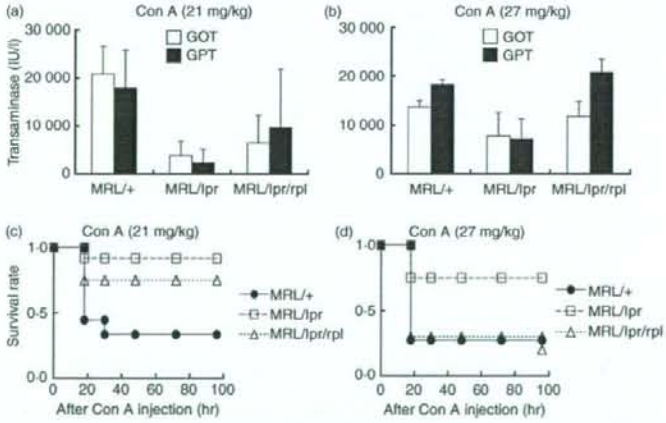

Figure 1. MRL/lpr/rpl mice are susceptible to concanavalin A (Con A)-induced hepatitis. MRL/+, MRL/lpr and MRL/lpr/rpl mice were injected with the indicated dose of Con A into the tail vein. Plasma transaminase levels were measured 12 hr after injection (a,b). Data are presented as mean + standard deviation (SD). MRL mice were injected with the indicated dose of Con A and their survival was monitored thereafter (c,d). GOT, glutamate oxalate transaminase; GPT, glutamic pyruvic transaminase.

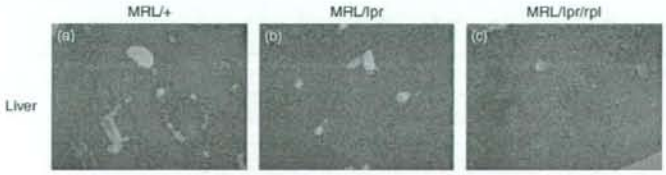

Figure 2. Histological analysis of the liver of MRL mice with induced hepatitis. Microscopic images of the livers of MRL/+ (a), MRL/lpr (b) and MRL/lpr/rpl (c) concanavalin A (Con A)-injected mice after haematoxylin and eosin staining.

with that from the transaminase and survival experiments. Thus, MRL/lpr/rpl mice are susceptible to Con A-induced hepatitis in a Fas-independent manner.

MRL/+/rpl mice are less sensitive to hepatitis

It was of interest to establish whether MRL/+/rpl mice are also susceptible to Con A-induced hepatitis. When 21 mg/kg of Con A was injected, severe hepatitis was induced in MRL/+ mice, but not in MRL/+/rpl mice (Fig. 3a,b). When 27 mg/kg of Con A was injected, severe hepatitis was also induced in MRL/+ mice. However, MRL/+/rpl mice were less sensitive than MRL/+ mice (Fig. 3c). Taken together, the results indicate that MRL/+/rpl mice were less sensitive to Con A-induced hepatitis, and this result was contrary to our expectations.

$CD4^+$ and $CD8^+$ T cells are responsible for the induction of hepatitis in MRL/lpr/rpl mice

We evaluated the role of $CD4^+$ and $CD8^+$ T and NK cells from MRL/+ mice in the induction of hepatitis in MRL/lpr/rpl mice. In MRL/+ mice, treatment with monoclonal anti-CD4 and anti-CD8 abrogated the induction of hepatitis caused by 21 mg/kg of Con A (Fig. 4a,b). Meanwhile, treatment with monoclonal anti-CD4 and anti-CD8 had only a slight effect on the induction of hepatitis in MRL/+ mice caused by 27 mg/kg of Con A (Fig. 4c). Interestingly, treatment of MRL/lpr mice with monoclonal anti-CD8 worsened the prognosis of hepatitis (Fig. 4d), suggesting the involvement of $CD8^+$ T cells in protection against hepatitis. In MRL/lpr/rpl mice, treatment with monoclonal anti-CD4 and anti-CD8 abrogated the induction of hepatitis caused by 27 mg/kg of Con A (Fig. 4e). Treatment with anti-asialo GM1 partially changed the susceptibility of MRL/lpr/rpl mice to hepatitis. Thus, the antibody-depletion study aided in the identification of effector cells in hepatitis induced in MRL/lpr/rpl mice.

Vα14 NKT cells were absent in MRL/lpr/rpl mice

It has been reported that Vα14 NKT cells are absent in SAP-deficient mice.[3] Because MRL/lpr/rpl mice are susceptible to hepatitis and Vα14 NKT cells are essential for the Con A-induced hepatitis, it was hypothesized that Vα14 NKT cells exist in MRL/lpr/rpl mice. It was suggested that Vα14 NKT precursor cells would be depleted in the absence of SAP-mediated signals in a Fas-dependent manner. Flow cytometric analysis of the hepatic mononuclear cells and splenocytes was performed to elucidate the existence of Vα14 NKT cells in MRL/lpr/rpl mice. Vα14 NKT cell numbers in MRL/lpr mice were reduced as reported previously,[19] and contrary to our expectations, Vα14 NKT cells did not exist in the liver or spleen of MRL/lpr/rpl mice (Fig. 5).

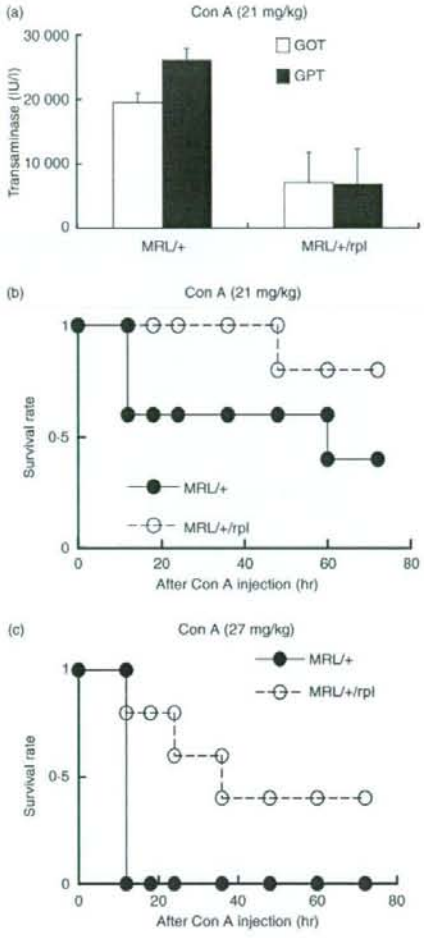

Figure 3. MRL/+/rpl mice are less sensitive to concanavalin A (Con A)-induced hepatitis. MRL/+ and MRL/+/rpl mice were injected with the indicated dose of Con A in the tail vein. Plasma transaminase levels were measured 12 hr after injection (a). Data are presented as mean + standard deviation (SD). MRL mice were injected with the indicated dose of Con A and the subsequent survival was monitored (b,c). GOT, glutamate oxalate transaminase; GPT, glutamic pyruvic transaminase.

IL-4 expression was not observed in hepatitis in MRL/lpr/rpl mice

The expression levels of IL-4 in Con A-induced hepatitis were analyzed. The levels of IL-4 were elevated in sera from MRL/+ mice but not in sera from MRL/lpr or MRL/lpr/rpl

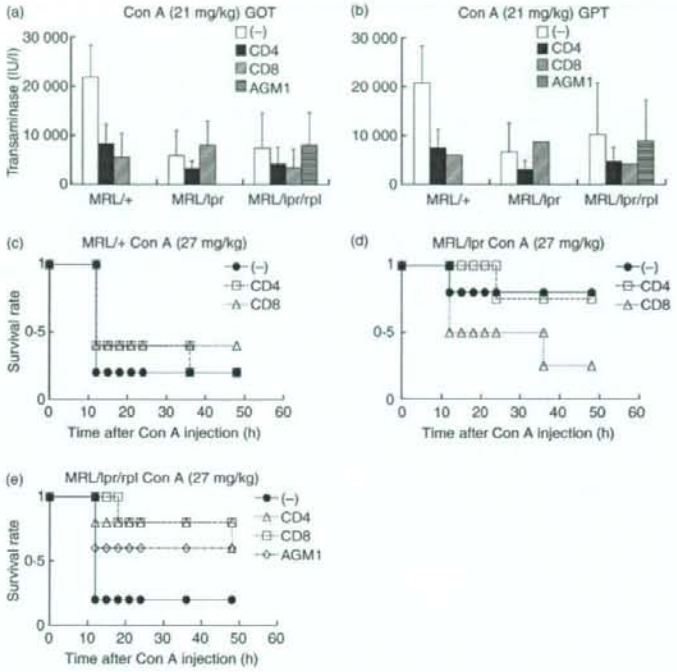

Figure 4. The development of hepatitis in MRL/lpr/rpl mice was mediated by $CD4^+$ and $CD8^+$ T cells. MRL/+, MRL/lpr and MRL/lpr/rpl mice were pretreated with monoclonal anti-CD4 (GK1·5) or anti-CD8 (53–6·72) or anti-asialo GM1 (AGM1) at 3, 2 and 1 day before injection with the indicated dose of concanavalin A (Con A) into the tail vein. Plasma transaminase levels were measured 12 hr after injection of Con A (a,b). Data are presented as mean + standard deviation (SD). MRL mice pretreated with the same antibodies were injected with the indicated dose of Con A and the subsequent survival was monitored (c–e). GOT, glutamate oxalate transaminase; GPT, glutamic pyruvic transaminase.

(Fig. 6a,b). The elevation of IL-4 correlated with the existence of Vα14 NKT cells but not with the induction of hepatitis, suggesting that IL-4 expression is not essential for the induction of hepatitis in MRL/lpr/rpl mice.

The 2B4 molecule is involved in hepatitis in MRL/lpr/rpl mice

To elucidate the role of the SLAM family receptor-mediated signals in MRL/lpr/rpl mice, hydrodynamic injection of plasmids was performed before the induction of hepatitis with 27 mg/kg of Con A (Fig. 7b). In the hepatitis model induced by the injection of 27 mg/kg of Con A, blockade of the 2B4–Fc fusion protein resulted in a significant decrease in plasma transaminase. On the contrary, blockade of the 2B4–Fc fusion protein in MRL/+ mice did not result in a significant decrease in plasma transaminase. In MRL/+ mice expressing CD84–Fc and SLAM–Fc fusion proteins, the GPT level was lower than in the other groups, but the GOT level was comparable (Fig. 7a). The

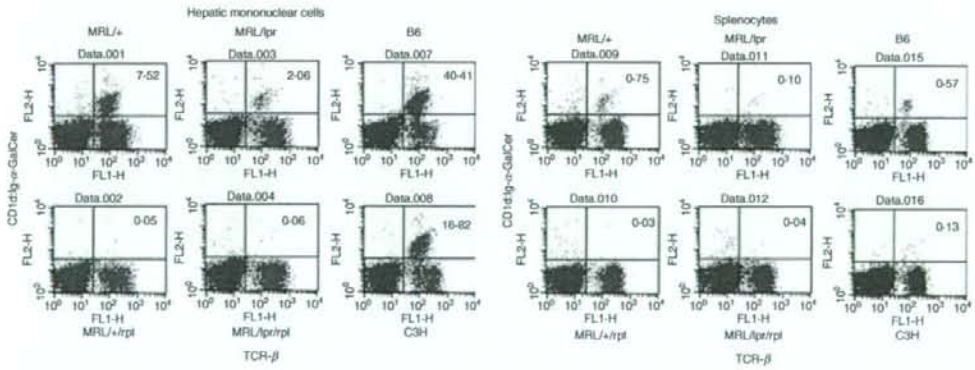

Figure 5. Vα14 NKT cells are absent in MRL/lpr/rpl mice. Hepatic mononuclear cells and splenocytes from MRL mice were stained with murine CD1d:Ig-α-galactosylceramide and monoclonal anti-T-cell receptor (TCR)β chain, and analyzed using a flow cytometer.

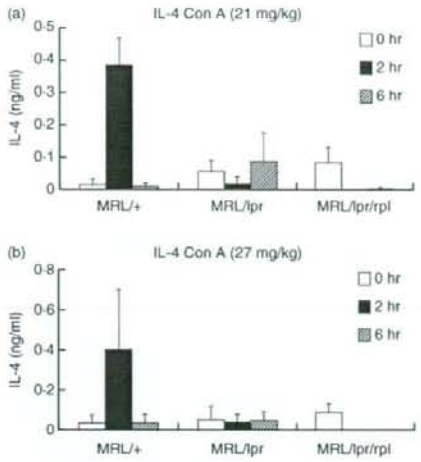

Figure 6. Hepatitis in MRL/lpr/rpl mice was not mediated by interleukin-4 (IL-4). MRL/+, MRL/lpr and MRL/lpr/rpl mice were injected in the tail vein with the indicated dose of concanavalin A (Con A). Serum IL-4 (a,b) levels were measured 0, 2 and 6 hr after injection. Data are presented as mean + standard deviation (SD).

expression of Fc fusion protein in the plasma of treated mice was confirmed in both MRL/+ and MRL/lpr/rpl mice (Fig. 7c). These data suggest that some lymphocyte populations expressing 2B4 are responsible for the induction of hepatitis in MRL/lpr/rpl mice.

Discussion

It is known that mice which lack Vα14 NKT cells and Fas-deficient mice are less sensitive to hepatitis.[7,9] However, in this study, we showed that MRL/lpr/rpl mice which lack Vα14 NKT cells and are deficient for the Fas antigen are sensitive to Con A-induced hepatitis. The hepatitis induced in MRL/lpr/rpl mice was Fas independent. One explanation for this phenomenon is that intravenously injected Con A was expended by the expanded population of lymphocytes, namely $CD4^-$ $CD8^-$ *lpr* T cells, in MRL/lpr mice, thus altering the susceptibility of the MRL/lpr mice. Because the number of *lpr* T cells was reduced in MRL/lpr/rpl mice,[17] these mice were susceptible to hepatitis. However, MRL/lpr mice treated with monoclonal anti-CD8 became susceptible to the hepatitis, even though the splenomegaly and lymphadenopathy were maintained in MRL/lpr mice after treatment with the monoclonal anti-CD8 (Fig. 4d). This finding is not consistent with the Con A-expending hypothesis. The next explanation is that Fas deficiency in the *lpr* mutant is leaky,[7,15] and Fas expressed at low levels mediates the apoptotic signals in hepatocytes of MRL/lpr/rpl mice. The expression of Fas was not detected in MRL/lpr mice or in MRL/lpr/rpl mice.[17] It was reported that the expression of Fas was induced in MRL/lpr mice by the administration of Con A.[7] Although expression of Fas was also induced in MRL/lpr/rpl mice, but not in MRL/lpr mice, the expression levels in MRL/lpr/rpl mice were comparable or relatively lower (expression levels of *Fas* from gene chip data of the spleen before and 3 hr after injection of

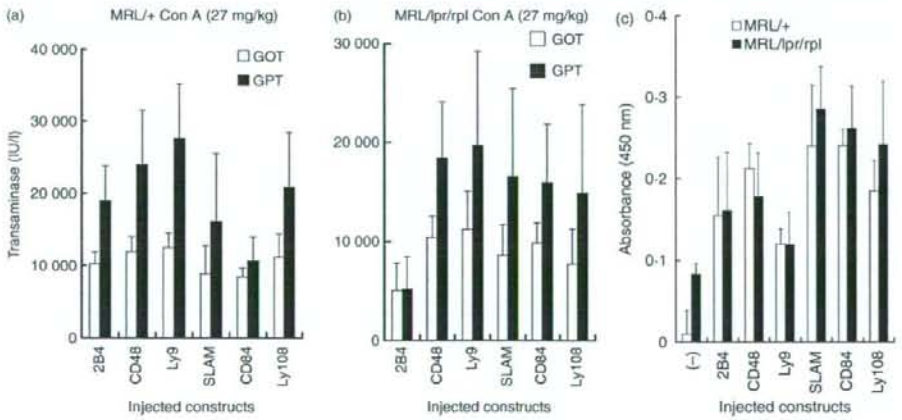

Figure 7. Hepatitis in MRL/lpr/rpl mice was mediated by $2B4^+$ T cells. MRL/+ and MRL/lpr/rpl mice were pretreated by hydrodynamic injection of the indicated plasmids and injected with the indicated dose of concanavalin A (Con A) into the tail vein 10 hr after injection with the plasmid. Plasma transaminase levels were measured 12 hr after injection with Con A (a,b). The expression of the Fc fusion protein in the plasma was confirmed by enzyme-linked immunosorbent assay (ELISA) (c). Data are presented as mean + standard deviation (SD). GOT, glutamate oxalate transaminase; GPT, glutamic pyruvic transaminase.

27 mg/kg of Con A: MRL/lpr: 187·2, 87·9; MRL/lpr/rpl: 25·2, 44·0). Therefore, this hypothesis cannot explain the difference in the susceptibility of the MRL/lpr and MRL/lpr/rpl strains. The other explanation is that the defects in Fas and SAP in MRL/lpr/rpl mice altered the development of some subpopulations of T cells and such newly developed lymphocytes caused the hepatitis instead of the Vα14 NKT cells. It has been reported that SAP deficiency causes a developmental defect in Vα14 NKT cells,[3] but it also causes a developmental defect in another subpopulation of T cells in a Fas-dependent manner. As treatment with monoclonal anti-CD4 and anti-CD8 abrogated the induction of hepatitis in MRL/lpr/rpl mice, and the blockade of 2B4 inhibited the induction of hepatitis in MRL/lpr/rpl mice (Fig. 7), 2B4 but not SAP-mediated signals in $2B4^+$ $CD4^+$ and $2B4^+$ $CD8^+$ T cells played important roles in the induction of the hepatitis in MRL/lpr/rpl mice. As a next step, we should identify which of the $2B4^+$ T-cell subpopulation was responsible for the induction of hepatitis.

The signals from 2B4 molecules were mediated in NK cells by SAP and SAP-related adaptors, Ewing's sarcoma-activated transcript-2 (EAT-2) and EAT-2-related transducer (ERT).[20] EAT-2 and ERT are known to mediate inhibitory signals in NK cells. It is still ambiguous whether the other SAP-related adaptor could be involved in transduction of the activating signals mediated from 2B4 in T cells in the hepatitis induced in MRL/lpr/rpl mice by Con A, even though the possibility of the presence of the other SAP-related adaptors has been raised.[21] The other SAP-related adaptor that can bind to 2B4 would transduce enhanced activating signals in the absence of SAP. However, the transducer of the 2B4-mediated signals in the hepatitis induced in MRL/lpr/rpl mice by Con A is still unknown and should be investigated further.

Vα14 NKT cells are known to be essential for the induction of hepatitis. As Vα14 NKT cells were absent in MRL/lpr/rpl mice (Fig. 5), the Con A-induced hepatitis in MRL/lpr/rpl mice was independent of Vα14 NKT cells. Instead of Vα14 NKT cells, MR-1-restricted Vα19 T cells, recently described as unconventional NKT cells,[22] were candidate $2B4^+$ T cells responsible for hepatitis induction. As the expansion of Vα19 NKT cells in Vα14 NKT-cell-deficient mice has been reported,[23] the number of Vα19 NKT cells could increase in Vα14 NKT-cell-deficient MRL/lpr/rpl mice. Future studies should be carried out to clarify whether this population is expanded in MRL/lpr/rpl mice and if it is responsible for the induction of hepatitis by Con A. It was also reported that expression of IL-4 was caused by Vα14 NKT cells and is essential for induction of the hepatitis.[11] In this study, IL-4 expression was not observed in the MRL/lpr/rpl mice with Con A-induced hepatitis (Fig. 6). This defect in IL-4 expression was a result of the absence of Vα14 NKT cells. Therefore, it is indicated that $2B4^+$ T cells cause hepatitis in MRL/lpr/rpl mice in an IL-4-independent manner. Taken together, the hepatitis induced in MRL/lpr/rpl mice was found to be independent of Fas, Vα14 NKT cells and IL-4, but dependent on signals mediated by adaptors other than SAP from 2B4 in T cells.

Acknowledgements

α-GalCer was provided by KIRIN brewery. We thank Dr Hiroyuki Nishimura (Wakayama Medical University) for fruitful discussions; Ms Fumiko Date, Ms Naoko Shibata and Ms Naomi Yamaki (Tohoku University) for providing technical assistance; and Ms Noriko Fujisawa and Ms Emi Yura (Tohoku University) for secretarial assistance. This study was supported by Grants-in-Aid for Scientific Research from the Ministry of Education, Science, Sports, and Culture of Japan to H.F. (#16790221) and M.O. (#16390113, 19390108 and 19659096).

References

1 Engel P, Eck MJ, Terhorst C. The SAP and SLAM families in immune responses and X-linked lymphoproliferative disease. *Nat Rev Immunol* 2003; **3**:813–21.
2 Sayos J, Wu C, Morra M *et al.* The X-linked lymphoproliferative-disease gene product SAP regulates signals induced through the co-receptor SLAM. *Nature* 1998; **395**:462–9.
3 Nichols KE, Hom J, Gong SY *et al.* Regulation of NKT cell development by SAP, the protein defective in XLP. *Nat Med* 2005; **11**:340–5.
4 Matsuda JL, Gapin L. Developmental program of mouse Valpha14i NKT cells. *Curr Opin Immunol* 2005; **17**:122–30.
5 Yu KO, Porcelli SA. The diverse functions of CD1d-restricted NKT cells and their potential for immunotherapy. *Immunol Lett* 2005; **100**:42–55.
6 Tiegs G, Hentschel J, Wendel A. A T cell-dependent experimental liver injury in mice inducible by concanavalin A. *J Clin Invest* 1992; **90**:196–203.
7 Tagawa Y, Kakuta S, Iwakura Y. Involvement of Fas/Fas ligand system-mediated apoptosis in the development of concanavalin A-induced hepatitis. *Eur J Immunol* 1998; **28**:4105–13.
8 Kaneko Y, Harada M, Kawano T, Yamashita M, Shibata Y, Gejyo F, Nakayama T, Taniguchi M. Augmentation of Valpha14 NKT cell-mediated cytotoxicity by interleukin 4 in an autocrine mechanism resulting in the development of concanavalin A-induced hepatitis. *J Exp Med* 2000; **191**:105–14.
9 Takeda K, Hayakawa Y, Van Kaer L, Matsuda H, Yagita H, Okumura K. Critical contribution of liver natural killer T cells to a murine model of hepatitis. *Proc Natl Acad Sci U S A* 2000; **97**:5498–503.
10 Tagawa Y, Sekikawa K, Iwakura Y. Suppression of concanavalin A-induced hepatitis in IFN-gamma(−/−) mice, but not in TNF-alpha(−/−) mice: role for IFN-gamma in activating apoptosis of hepatocytes. *J Immunol* 1997; **159**:1418–28.
11 Toyabe S, Seki S, Iiai T *et al.* Requirement of IL-4 and liver NK1+ T cells for concanavalin A-induced hepatic injury in mice. *J Immunol* 1997; **159**:1537–42.

12 Massaguer A, Perez-Del-Pulgar S, Engel P, Serratosa J, Bosch J, Pizcueta P. Concanavalin-A-induced liver injury is severely impaired in mice deficient in P-selectin. *J Leukoc Biol* 2002; **72**:262–70.

13 Diao H, Kon S, Iwabuchi K *et al.* Osteopontin as a mediator of NKT cell function in T cell-mediated liver diseases. *Immunity* 2004; **21**:539–50.

14 Anand S, Wang P, Yoshimura K *et al.* Essential role of TNF family molecule LIGHT as a cytokine in the pathogenesis of hepatitis. *J Clin Invest* 2006; **116**:1045–51.

15 Adachi M, Watanabe-Fukunaga R, Nagata S. Aberrant transcription caused by the insertion of an early transposable element in an intron of the Fas antigen gene of lpr mice. *Proc Natl Acad Sci USA* 1993; **90**:1756–60.

16 Watanabe-Fukunaga R, Brannan CI, Copeland NG, Jenkins NA, Nagata S. Lymphoproliferation disorder in mice explained by defects in Fas antigen that mediates apoptosis. *Nature* 1992; **356**:314–7.

17 Komori H, Furukawa H, Mori S *et al.* A signal adaptor SLAM-associated protein regulates spontaneous autoimmunity and Fas-dependent lymphoproliferation in MRL-Faslpr lupus mice. *J Immunol* 2006; **176**:395–400.

18 Yang JQ, Singh AK, Wilson MT *et al.* Immunoregulatory role of CD1d in the hydrocarbon oil-induced model of lupus nephritis. *J Immunol* 2003; **171**:2142–53.

19 Yang JQ, Saxena V, Xu H, Van Kaerl., Wang CR, Singh RR. Repeated alpha-galactosylceramide administration results in expansion of NK T cells and alleviates inflammatory dermatitis in MRL-lpr/lpr mice. *J Immunol* 2003; **171**: 4439–46.

20 Veillette A. NK cell regulation by SLAM family receptors and SAP-related adapters. *Immunol Rev* 2006; **214**:22–34.

21 Veillette A. Immune regulation by SLAM family receptors and SAP-related adaptors. *Nat Rev Immunol* 2006; **6**:56–66.

22 Kawachi I, Maldonado J, Strader C, Gilfillan S. MR1-restricted V alpha 19i mucosal-associated invariant T cells are innate T cells in the gut lamina propria that provide a rapid and diverse cytokine response. *J Immunol* 2006; **176**: 1618–27.

23 Croxford JL, Miyake S, Huang YY, Shimamura M, Yamamura T. Invariant V(alpha)19i T cells regulate autoimmune inflammation. *Nat Immunol* 2006; **7**:987–94.

殻付き微細気泡群を含む液体中における非線形波の伝播

Propagation of Nonlinear Wave in Liquid Containing Encapsulated Microbubbles

○金川 哲也, 北大工, 札幌市北区北 13 条西 8 丁目, E-mail: kanagawa@mech-me.eng.hokudai.ac.jp
矢野　猛, 阪大工, 吹田市山田丘 2-1, E-mail: yano@mech.eng.osaka-u.ac.jp
渡部 正夫, 北大工, 札幌市北区北 13 条西 8 丁目, E-mail: masao.watanabe@eng.hokudai.ac.jp
藤川 重雄, 北大工, 札幌市北区北 13 条西 8 丁目, E-mail: fujikawa@eng.hokudai.ac.jp

Tetsuya Kanagawa, Graduate School of Engineering, Hokkaido University, Sapporo 060-8628
Takeru Yano, Graduate School of Engineering, Osaka University, Suita 565-0871
Masao Watanabe, Graduate School of Engineering, Hokkaido University, Sapporo 060-8628
Shigeo Fujikawa, Graduate School of Engineering, Hokkaido University, Sapporo 060-8628

One-dimensional nonlinear waves in a liquid containing a number of spherical microbubbles are theoretically studied on the basis of a two-fluid model equations. The set of averaged equations consists of conservation laws of mass and momentum in gas and liquid phases, and the equation of motion of bubble wall. The compressibility of liquid phase is taken into account in the conservation laws and the equation of bubble wall motion, and this leads to the wave attenuation due to bubble oscillations. By using the method of multiple scales, Korteweg-de Vries-Burgers equation can be derived. The properties of the equation are discussed and compared to previous results based on different models on bubbly liquids.

1. はじめに

薬剤を内部に封入した殻付き微細気泡を患部近傍へと運搬させた後, 超音波照射によって殻の破壊を誘起させ, 薬剤を患部へ作用させるという, ドラッグデリバリーを利用した非侵襲がん治療技術 [1] が注目されている. 臨床現場においては, 殻の破壊を誘起させうるほどに強力な超音波を用いるといった観点から, そのふるまいを線形領域で把握することは不可能であり, 気泡振動と音波の非線形相互作用を詳細に把握することが強く望まれている. 本稿では, その最も基礎的な知見を得るために, 多数の微細気泡 (殻を有しない) を含む液体中を伝播する弱非線形波動に取り組む.

気泡流中を伝播する非線形波動に関する解析的研究は, 古くから多様な事例が報告されており, たとえば, 支配方程式系を分散性をともなう単一の非線形方程式である Korteweg-de Vries 方程式へと帰着させた研究 [2], さらに, これに粘性に起因する散逸性をも含めて K-dV-Burgers 方程式へと帰着させた例 [3] などが挙げられよう. しかしながら, これらの報告は, 液相を非圧縮性とみなすこと, また気相および液相の圧力を単一の変数として取り扱う (表面張力の無視) ことなど, 大胆ともいえる仮定の下での結果であり, 気泡流中を伝播する非線形波の精密な理解にはそぐうものではない. このように, 気泡流を記述するための従属変数の多さなどに起因する理論解析の困難さに阻まれ, その基礎的な知見ですら, いまだ不明瞭といえる状況にある.

本研究では, 体積平均化に基づく気泡流の支配方程式系を起点として, 初期に一様に気泡を含む圧縮性液体中を伝播する非線形波動を理論的に取り扱う. Egashira らによって提出された 3 圧力 2 流体モデルに基づく平均化方程式系 [4] は, 液相および気相の圧力, 密度, 流速にそれぞれ異なる従属変数を導入する点, なかでも圧力に対しては気相と液相の両者のみならず, 気泡の非線形振動によって誘起される気泡近傍液体の局所的高圧 (気液界面における液相圧力) をも, 単独の従属変数として組み込みうるという点で特徴的である. この方程式系を起点として, 静止液体中および気泡流中を伝播する線形分散波の解析がなされてきており [4][5], 本稿ではその非線形領域への拡張が実行される. 特異摂動法の利用, また従属変数群の 2 次までの展開を行った結果, 支配方程式系が, 圧縮性液体中での気泡振動に起因する分散ならびに散逸効果, また 2 次の非線形効果を記述しうる, 気泡径の摂動項を従属変数とする単一の Korteweg-de Vries-Burgers 方程式へと帰着されることが示される.

2. 問題の定式化

初期時刻において, 気泡径やボイド率を含むすべての物理量が一様状態にあるとする, 多数の球形微細気泡を含む静止液体を想定する. 液体中に設置された音源の振動によって平面音波が放射されている. 音波の波面に直交する方向に空間座標 x をとる (座標の原点 O を初期時刻における音源の位置に設置する) ことによって, 空間依存性が 1 次元とみなせる問題に定式化できる.

本解析において, とくに着目されるのは液相の圧縮性であり, その結果, 音響放射減衰 (気泡の非線形振動に起因) に基づく散逸効果の抽出などが帰着する. そのような観点から, 簡単のため, 液相と気相の粘性および熱伝導性, 気液界面を通じての熱および物質移動, 相変化, また体積力の存在は無視する. さらに, 気泡は任意の時刻および位置において球形を保ち, 合体, 分裂, 生成, 消滅は起こらないものとする.

2.1 基礎方程式系

波動伝播の解析に先立って, 気泡流の運動を支配する方程式系を導入してゆく. 本項で導入される諸変数および諸定数は, すべて無次元化されており, その定義は, のちの 2.2 項において詳述される.

気泡流の運動は, 質量および運動量の保存則を表す以下の体積平均化に基づく方程式系 [4] にしたがうものとする:

- 気相の質量保存則

$$\frac{\partial}{\partial t}(\alpha\rho_G) + \frac{\partial}{\partial x}(\alpha\rho_G u_G) = 0. \tag{1}$$

- 液相の質量保存則

$$\frac{\partial}{\partial t}[(1-\alpha)\rho_L] + \frac{\partial}{\partial x}[(1-\alpha)\rho_L u_L] = 0. \tag{2}$$

- 気相の運動量保存則

$$\frac{\partial}{\partial t}(\alpha\rho_G u_G) + \frac{\partial}{\partial x}\left(\alpha\rho_G {u_G}^2\right) + \kappa\alpha\frac{\partial p_G}{\partial x} = F. \quad (3)$$

- 液相の運動量保存則

$$\frac{\partial}{\partial t}\left[(1-\alpha)\rho_L u_L\right] + \frac{\partial}{\partial x}\left[(1-\alpha)\rho_L u_L^2\right] + \kappa(1-\alpha)\frac{\partial p_L}{\partial x} + \kappa P\frac{\partial \alpha}{\partial x} = -F. \quad (4)$$

ここに, t は時間, α は気相の体積率 (ボイド率), u は流速, ρ は流体の密度, p は圧力, P は気液界面における局所的な液相圧力であり, また下添え字 G と L は, それぞれ, 気相および液相に付随する体積平均化された変数を意味する.

運動量保存則 (3)(4) における, 相間の運動量輸送項 F としては, 液相の圧縮性を考慮できるように拡張された付加慣性力 [6]

$$F = -\beta_1\alpha\rho_L\left(\frac{D_G u_G}{Dt} - \frac{D_L u_L}{Dt}\right) - \beta_2\rho_L(u_G - u_L)\frac{D_G\alpha}{Dt} - \beta_3\alpha(u_G - u_L)\frac{D_G\rho_L}{Dt}, \quad (5)$$

を導入する. 係数 $\beta_1, \beta_2, \beta_3$ は, 通常すべて $1/2$ とおかれることが多いが, 本稿では具体的な値を与えずに式展開を進めてゆく.

また, 気相および液相に沿う Lagrange 微分 D_G/Dt および D_L/Dt は, それぞれ, 以下のように定義される演算子である:

$$\frac{D_G}{Dt} \equiv \frac{\partial}{\partial t} + u_G\frac{\partial}{\partial x}, \qquad \frac{D_L}{Dt} \equiv \frac{\partial}{\partial t} + u_L\frac{\partial}{\partial x}. \quad (6)$$

気泡の運動方程式として, 液相の圧縮性を考慮に含む Keller の方程式 [7] を導入する:

$$\left(1 - M\delta\frac{D_G R}{Dt}\right)R\frac{D_G^2 R}{Dt^2} + \frac{3}{2}\left(1 - \frac{M\delta}{3}\frac{D_G R}{Dt}\right)\left(\frac{D_G R}{Dt}\right)^2 = \frac{\kappa}{\delta^2}\left(1 + M\delta\frac{D_G R}{Dt}\right)P + \frac{M\kappa}{\delta}R\frac{D_G}{Dt}(p_L + P). \quad (7)$$

ここで, R は気泡径であり, また無次元パラメータである M, δ, κ の定義については 2.2 項において後述される. 式 (7) の導入に関して, 単一気泡を扱った原著 [7] においては, 1 変数の時間に関する導関数で表されていた項の演算子を D_G/Dt で置き換え, また, 気液界面における局所液相圧力 P の導入も行うなどの操作を経ている.

方程式系 (1)-(4) および (7) は, 以下に示す 4 つの補助的関係式を導入することによって閉じられる. まず, 熱力学的状態変数を関係づける式として, 気相にはポリトロープ変化の関係式

$$\frac{p_G}{p_{G0}} = \left(\frac{\rho_G}{\rho_{G0}}\right)^\gamma, \quad (8)$$

を (p_{G0} と ρ_{G0} は, それぞれ, 気相の初期圧力と初期密度, γ は気泡内気体のポリトロープ指数), 液相には Tait 型の状態方程式

$$\frac{p_L + B}{1 + B} = \rho_L^n, \quad (9)$$

をそれぞれ課す (B および n は物質定数). さらに, 気泡内気体の質量保存則

$$\rho_G R^3 = \rho_{G0}, \quad (10)$$

また, 気液界面でにおける圧力のつりあい (Laplace の式)

$$p_G - (p_L + P) = \frac{2\sigma}{R}, \quad (11)$$

を導入する (σ は表面張力).

9 本の式から構成される方程式系 (1)-(4) および (7)-(11) は, 9 つの従属変数 $\alpha, \rho_G, \rho_L, u_G, u_L, p_G, p_L, P, R$ に対して, 閉じた方程式系を形成している.

2.2 無次元化の定義

方程式系 (1)-(11) における諸変数は, すでに, 以下の定義にしたがって無次元化されている:

$$x = \frac{x^*}{L^*}, \quad t = \frac{U^* t^*}{L^*}, \quad u_G = \frac{u_G^*}{U^*}, \quad u_L = \frac{u_L^*}{U^*},$$
$$\rho_G = \frac{\rho_G^*}{\rho_{L0}^*}, \quad \rho_L = \frac{\rho_L^*}{\rho_{L0}^*}, \quad p_G = \frac{p_G^*}{p_{L0}^*},$$
$$p_L = \frac{p_L^*}{p_{L0}^*}, \quad P = \frac{P^*}{p_{L0}^*}, \quad R = \frac{R^*}{R_0^*}. \quad (12)$$

ここで, L^*, U^* はそれぞれ流れ場 (音場) の代表的な長さ, 速さスケールであり, これらに加え, 液相の有次元の初期密度と初期圧力 ρ_{L0}^*, p_{L0}^* および初期の気泡径 R_0^* を用いて無次元化を行っている. アスタリスク "$*$" を, すべての, 有次元変数および有次元定数に記してあることに注意されたい.

つづいて, 無次元諸定数の定義も示す:

$$\rho_{G0} = \frac{\rho_{G0}^*}{\rho_{L0}^*}, \quad p_{G0} = \frac{p_{G0}^*}{p_{L0}^*}, \quad B = \frac{B^*}{p_{L0}^*}, \quad \sigma = \frac{\sigma^*}{p_{L0}^* R_0^*}. \quad (13)$$

さらに, 無次元方程式系 (3)(4) および (7) に現れているパラメータ κ, M, δ は, 以下の定義によって導入されたものである:

$$\kappa = \frac{p_{L0}^*}{\rho_{L0}^* U^{*2}}, \quad M = \frac{U^*}{c_{L0}^*}, \quad \delta = \frac{R_0^*}{L^*}. \quad (14)$$

ここに, c_{L0}^* は初期の液単相音速であり, また, δ とは流れ場の代表長さスケール (たとえば波長) に対する初期気泡径の比をあらわす.

ここで, 平均化方程式系を用いるにあたって重要となる空間スケールについて触れておく. 気泡流中の 4 つの長さスケール, すなわち, 気泡径, 気泡間距離, 平均化の長さスケール, 流れ場の代表長さスケール, これらについて, 以下の大小関係が成立していなければならない:

$$R_0^* \ll {n_0^*}^{-1/3} \ll {V^*}^{1/3} \ll L^*. \quad (15)$$

ここに, n_0^* は初期の気泡数密度 (したがって ${n_0^*}^{-1/3}$ とは初期の気泡間距離), V^* は平均化体積である. 不等式 (15) とは, 気泡半径が十分小さく, 平均化体積内に十分たくさんの気泡が含まれていて, かつ, 注目する波の運動スケールが平均化のスケールより大きいという要請である. したがって

$$\alpha_0 = \frac{4}{3}\pi {R_0^*}^3 n_0^* \ll 1, \quad (16)$$

なる関係が成立する. すなわち, 初期ボイド率 α_0 は, 1 に比べて十分に小さくなければならない.

3. 非線形波動を記述する単一方程式への帰着

3.1 摂動展開

方程式系 (1)-(4) および (7)-(11) における, 9 つの従属変数に対して, その大きさが $0 < \epsilon \ll 1$ とみなせるパラメータ ϵ を用いて, 以下のような展開をおこなう:

$$u_G = \epsilon u_{G1} + \epsilon^2 u_{G2} + \cdots, \quad (17)$$
$$u_L = \epsilon u_{L1} + \epsilon^2 u_{L2} + \cdots, \quad (18)$$
$$\rho_G = \rho_{G0}(1 + \epsilon\rho_{G1} + \epsilon^2\rho_{G2} + \cdots), \quad (19)$$

$$\rho_L = 1 + \epsilon\rho_{L1} + \epsilon^2\rho_{L2} + \cdots, \tag{20}$$
$$p_G = p_{G0}(1 + \epsilon p_{G1} + \epsilon^2 p_{G2} + \cdots), \tag{21}$$
$$p_L = 1 + \epsilon p_{L1} + \epsilon^2 p_{L2} + \cdots, \tag{22}$$
$$P = \epsilon P_1 + \epsilon^2 P_2 + \cdots, \tag{23}$$
$$R = 1 + \epsilon R_1 + \epsilon^2 R_2 + \cdots, \tag{24}$$
$$\alpha = \alpha_0(1 + \epsilon\alpha_1 + \epsilon^2\alpha_2 + \cdots). \tag{25}$$

ここで，たとえば，u_{G1}, u_{G2} などといった従属変数群の摂動項は，すべて $O(1)$ であると定める．

つづいて，従属変数群の摂動項，たとえば，気泡径 R の 1 次および 2 次の摂動項に関して，以下のような独立変数依存性を仮定する (他の従属変数に関しても同様)：

$$R_1 = R_1(x, t_0, t_1), \qquad R_2 = R_2(x, t_0). \tag{26}$$

ここに，時間に関する独立変数について，t_0 と t_1 の両者が用意されているが，これらはそれぞれ

$$t_0 \equiv t, \qquad t_1 \equiv \epsilon t, \tag{27}$$

によって導入したものである．$\epsilon \ll 1$ であることから，$t_1 = \epsilon t$ とは，$t_0 = t$ にくらべて十分にゆるやかな (小さい) 変化を記述するのに適切な変数であることがわかる．定義 (27) から，R_1 の t に関する偏導関数は以下のように展開される：

$$\frac{\partial R_1}{\partial t} = \frac{\partial R_1}{\partial t_0} + \epsilon\frac{\partial R_1}{\partial t_1}. \tag{28}$$

時間に関して，t_0 に支配される方程式 (あるいは項) は，近傍場，すなわち解のふるまいがほぼ線形とみなせるような領域を記述し，いっぽう t_1 に支配される方程式は，遠方場，すなわち蓄積した弱い非線形効果が無視できないような領域を記述する．具体的には，近傍場を記述する線形方程式が 3.3 項で，遠方場を記述する非線形方程式が 3.4 項において，それぞれ導かれる．

3.2 諸変数と諸定数のオーダー設定

式 (13) や (14) などにおいてあらわれる，無次元諸定数およびパラメータのオーダーを設定する：

$$\begin{aligned} &\rho_{G0} = O(\epsilon^2), \quad p_{G0} = O(1), \quad \alpha_0 = O(1), \\ &B = O(1), \quad \sigma = O(1), \\ &M = O(\sqrt{\epsilon}), \quad \delta = O(\sqrt{\epsilon}), \quad \kappa = O(1). \end{aligned} \tag{29}$$

ここで，式 (29) における，$O(1)$ 以外の定数については

$$\delta \equiv \sqrt{\epsilon}\ \ {}_1, \quad M \equiv \sqrt{\epsilon}\ \ {}_2, \quad \rho_{G0} \equiv \epsilon^2\ \ {}_3, \tag{30}$$

とおいておく (${}_1 = O(1)$, ${}_2 = O(1)$, ${}_3 = O(1)$ とする)．なお，本問題で着目する現象は，最大で 2 次の摂動項が寄与するものであるため，ρ_{G0} からの寄与はないことは容易にわかる．

以上より，もともとの従属変数群 (17)-(25) のオーダーを，以下のように見積もったこととなる：

$$\begin{aligned} &u_G = O(\epsilon), \quad u_L = O(\epsilon), \quad \rho_G = O(\epsilon^2), \\ &\rho_L = O(1), \quad p_G = O(1), \quad p_L = O(1), \\ &P = O(\epsilon), \quad R = O(1), \quad \alpha = O(1). \end{aligned} \tag{31}$$

まず，ϵ^0 を係数とする関係式として，式 (9) および (11) から，ただちに以下の関係式群を得る：

$$c_{L0}^2 = \kappa n(1 + B), \qquad p_{G0} - 1 = 2\sigma. \tag{32}$$

ここに，$c_{L0} = c_{L0}^*/U^*$ は液単相の無次元初期音速である．

3.3 線形波動

保存則 (1)-(4) および Keller の方程式 (7) から，ϵ を係数とする項のみを取り出す．さらに，変数の削減のために，補助関係式 (8)-(11) を適切に用いれば，$\alpha_1, u_{G1}, u_{L1}, p_{L1}, R_1$ のみを未知変数とする方程式系を得る：

$$\frac{\partial\alpha_1}{\partial t_0} - 3\frac{\partial R_1}{\partial t_0} + \frac{\partial u_{G1}}{\partial x} = 0, \tag{33}$$
$$\frac{\kappa}{c_{L0}^2}\frac{\partial p_{L1}}{\partial t_0} - \frac{\alpha_0}{1-\alpha_0}\frac{\partial\alpha_1}{\partial t_0} + \frac{\partial u_{L1}}{\partial x} = 0, \tag{34}$$
$$\beta_1\frac{\partial u_{G1}}{\partial t_0} - \beta_1\frac{\partial u_{L1}}{\partial t_0} - 3\gamma\kappa p_{G0}\frac{\partial R_1}{\partial x} = 0, \tag{35}$$
$$\frac{1-\alpha_0+\beta_1\alpha_0}{1-\alpha_0}\frac{\partial u_{L1}}{\partial t_0} - \frac{\beta_1\alpha_0}{1-\alpha_0}\frac{\partial u_{G1}}{\partial t_0} + \kappa\frac{\partial p_{L1}}{\partial x} = 0, \tag{36}$$
$$p_{L1} + \omega_B^2 R_1 = 0. \tag{37}$$

ここに，$\omega_B^2 = 3\gamma p_{G0} - 2\sigma = O(1)$ は，単一気泡の無次元固有角振動数である．

方程式系 (33)-(37) は，いくらかの計算を経て，単一変数 R_1 に対する線形波動方程式

$$\frac{\partial^2 R_1}{\partial t_0^2} - v_p^2\frac{\partial^2 R_1}{\partial x^2} = 0, \tag{38}$$

へと帰着させることができる．これが近傍場を記述する方程式である．ここに，v_p は位相速度であり，$\alpha_0, \kappa, \omega_B$ などといった $O(1)$ の諸定数を用いて表現される (本稿ではその依存形は省略する)．

3.4 分散性と散逸性をあわせもつ非線形波動

式 (38) における位相速度を用いて，新たな独立変数 φ を

$$\varphi \equiv x - v_p t_0, \tag{39}$$

によって導入すれば，時間 t_0 および空間座標 x に対する偏微分演算子が，以下のように変数変換される：

$$\frac{\partial}{\partial t_0} = -v_p\frac{\partial}{\partial\varphi}, \qquad \frac{\partial}{\partial x} = \frac{\partial}{\partial\varphi}. \tag{40}$$

したがって，このとき仮に，従属変数が R_1 以外であっても，線形波動方程式 (38) の左辺は恒等的にゼロとなる．変数 φ の導入とは，x 軸正方向へと一定速度 v_p で進行する波の存在の仮定に対応する．また，式 (26) を，以下のように表現し直しておく：

$$R_1 = R_1(\varphi, t_1), \qquad R_2 = R_2(\varphi). \tag{41}$$

遠方場を記述する方程式を抽出するために，方程式系 (1)-(4) および (7) から，ϵ^2 を係数とする項を取り出し，3.3 項と同じく変数の削減も行うことによって，以下の方程式系を得る：

$$\frac{\partial}{\partial\varphi}[u_{G2} - v_p(\alpha_2 - 3R_2)] = f_1, \tag{42}$$
$$\frac{\partial}{\partial\varphi}\left[u_{L2} - v_p\left(\frac{\kappa}{c_{L0}^2}p_{L2} - \frac{\alpha_0}{1-\alpha_0}\alpha_2\right)\right] = f_2, \tag{43}$$
$$\frac{\partial}{\partial\varphi}[v_p\beta_1(u_{L2} - u_{G2}) - 3\gamma\kappa p_{G0}R_2] = f_3, \tag{44}$$
$$\frac{\partial}{\partial\varphi}\left[\kappa p_{L2} - \frac{v_p\{(1-\alpha_0+\beta_1\alpha_0)u_{L2} - \beta_1\alpha_0 u_{G2}\}}{1-\alpha_0}\right] = f_4 \tag{45}$$
$$p_{L2} + \omega_B^2 R_2 = f_5. \tag{46}$$

方程式系 (42)-(46) は，3.3 項の手順に倣えば，気泡径の 1 次摂動項 R_1 を従属変数とする単一方程式にまとめあげることが可能である．その際，以下の事項を用いて計算をすすめる：